ELSEVIER

Colloids and Surfaces
A: Physicochemical and Engineering Aspects 105 (1995) 47–77

COLLOIDS AND SURFACES A

The surface structure and reactivity of black carbon

D.M. Smith *, A.R. Chughtai

Department of Chemistry, University of Denver, Denver, CO 80208, USA

Received 1 March 1995; accepted 10 July 1995

Abstract

Fourier transform infrared (FT-IR) spectroscopy has been the most definitive analytical tool in a comprehensive program on the structure and reactivity of black carbon (in the form of *n*-hexane soot). In combination with other techniques, it has revealed the soot structure, as produced by high temperature incomplete combustion, to be predominantly aromatic with a surface coverage by oxygen-containing functional groups of about 0.5. Particularly well suited to following net changes in surface groups, and gas phase reactant/product concentrations, FT-IR has been the key technique in determining the kinetics and mechanisms of some important heterogeneous reactions of black carbon with gas phase oxidant molecules. For example, the reaction of NO_2/N_2O_4 with soot follows a dual path mechanism, down to 2 p.p.m., which is reflected in the rate law: initial rate $= (k_1 + k_2\,[\text{soot}]^{1/2})\,P_{NO2}$. On the other hand, catalytic decomposition initiates the reaction with ozone, followed by the formation of surface carboxylic groups and gaseous CO_2 and H_2O. The evidence suggests that dissociation of ozone yields a steady-state concentration of excited oxygen atom which is actually the oxidant. FTIR combined with chemical measurements has proven that a high solubility observed for carbon particles exposed to ozone has its origin in the hydrolysis of the surface carboxylics. Significant effects of simulated solar radiation on the reactions, especially in the soot/$SO_2/H_2O/O_2$ system, has been revealed by FTIR. Infrared will continue its central role in the examination of increasingly complex systems containing black carbon, particularly through its interface with ancillary techniques.

Keywords: Black carbon; FT-IR spectroscopy; Nitrogen dioxide; Ozone; Sulfur dioxide

1. Introduction

The purpose of this article is to describe the applications of infrared spectroscopy to studies of the surface structure and reactivity of black carbon, a ubiquitous environmental agent, which have been pursued by this research group in recent years. Although other analytical techniques, some of them spectroscopic, have been employed in this research, it is Fourier Transform Infrared (FT-IR) spectroscopy which possesses those characteristics required for definitive qualitative and quantitative structural and dynamics measurements in black carbon-containing systems. These and similar studies are providing important basic knowledge which ultimately will be necessary for an understanding of complex tropospheric systems involving carbonaceous particles.

Of both natural and anthropogenic origin, emissions of black carbon recently have been estimated at 24 Tg per year [1]. Source contributions to global fluxes from biomass burning, fossil fuel combustion and commercial production have been estimated in several ways [1–4], including studies of urban and regional airs. The mobilization of black carbon over long distances in the atmosphere has been revealed by a number of studies, including

* Corresponding author.

SSDI 0927-7757(95)03337-8

historic and prehistoric burning [5] as well as more recent measurement of arctic haze profiles [6,7], for example.

Carbon particles, alone and as components of atmospheric aerosol, have the potential to impact our biosphere in several ways. The earth's radiation budget is strongly affected by the single scattering albedo for solar radiation of tropospheric carbonaceous particles, as is visibility reduction. Fossil fuel-generated soot, especially in urban areas, is believed to underlie much human respiratory disease and tens of thousands of deaths annually. The reactivity of soot with such gas phase oxidant species as NO_2, O_3 and SO_2 has been documented by numerous laboratory and field studies (see for example, Ref. [8]) and thus generally is considered to have a role in tropospheric chemistry. It is the latter of these impacts, stimulated originally by the demonstration of a global distribution of black carbon through an aeolian transport mechanism [5], which has been the object of the research reviewed below.

Infrared spectroscopy has been employed in the study of solid carbonaceous materials, including coal, since at least 1945 [9–13]. The first interpretable infrared spectra of activated carbon and graphite were reported by Friedel and coworkers [14,15], however, in 1970–71. Extensive grinding of these intractable materials made possible the observation of infrared absorption bands in the 1700 cm^{-1}, 1600 cm^{-1} and 1200 cm^{-1} regions which now are recognized as generally characteristic of oxidized microcrystalline carbons. This work stimulated us [16], then in the laboratories of E.D. Goldberg, to investigate the functionalities responsible for infrared absorptions, from which the dependence of a characteristic 1585–1600 cm^{-1} band on oxygen was revealed through grinding experiments. A linear relationship between the integrated absorbance, $\int A(\nu)d\nu$, of this band and the mass of carbon was the basis for the development of an analytical method for the measurement of "elemental" carbon in pelagic ocean sediments [5]. Other infrared studies of carbonaceous materials containing elemental carbon have ensued, including those of the black carbon, in the form of *n*-hexane soot, described herein.

Nearly as many band assignments for the characteristic carbon absorptions have been made as there have been spectroscopists studying this intriguing material. Thus, the surface of particulate carbon has been described in terms of a variety of oxygen-containing functionalities whose existence has been postulated. These assignments [11–20] include alcohols, phenols, carbonyls, carboxylics, esters, ethers, quinones, hydroquinones, lactols, and lactones.

The soot produced by the high temperature incomplete combustion of carbonaceous fuels, in the case of hydrocarbons, is produced according to

$$C_xH_y + zO_2 = 2zCO + (y/2)H_2 + (x-2z)C \qquad (1)$$

For *n*-hexane, chosen as a model for liquid fossil fuels early in our research program [21], $x=6$ and $y=14$. The importance of structure and reactivity studies being referred to a single standard material cannot be overemphasized. The choice of *n*-hexane, a smooth-burning liquid with physical properties allowing easy handling and without unsaturated chemical functionalities, was made after examination of the characteristics of 30 potential fuel models. The use of *n*-hexane soot as a reference material has been supported by the work of others [22].

The long range goal of this research program, as noted above, is to provide a clearer understanding of the role of black carbon in tropospheric chemistry. Since the particulate surface structure, including chemical functionality, undoubtedly underlies that role, infrared spectroscopy has been a definitive tool in revealing that structure and in determining the kinetics and mechanisms of its heterogeneous reactions.

2. Experimental

2.1. Equipment

Energy limitations of dispersive infrared spectrometers impose constraints on the applicability of the technique to such energy absorbing and scattering materials as the black carbon derived from fossil fuel combustion. The trade-offs of slow scan or integration times to achieve acceptable

signal-to-noise ratios (S/N) and energy levels make the measurements of trace components, transient species or rapid reactions problematical with such instruments. FT-IR instruments have lifted these constraints and allowed the application of infrared spectroscopy to study the structure and follow the reactions of black carbon.

Digilab/Biorad FTS-20 and FTS-14B FT-IR Spectrometers were used, with three generations of computer and interface upgrades, for all infrared measurements. The current configuration was accomplished in house and employs a Micro Q 486 modified with Keithley Metrabyte digital and analog/digital interface boards, HP laser Jet IIIP printer/plotter, and color monitor. A combination of custom and off-the-shelf software is used to operate the system. Details of this data system and its spectrometer interface are to be found in a recent article [23] and also may be obtained directly from the corresponding author.

Infrared spectra of black carbon have been obtained primarily in the "transmission" mode, really a diffuse forward-reflectance technique [24], in which the light beam is passed through an infrared-transparent support material on which soot has been collected from the flame. Because of the particle size, scattering albedo and high absorptivity of *n*-hexane soot, it often is difficult to observe spectral detail in the region above 3000 cm^{-1} using this technique. One version of a cell for in-situ measurements of black carbon under various conditions of temperature and pressure, and for certain reaction rate measurements, is shown in Fig. 1 [25]. Horizontally and vertically mounted versions of this cell, fitted to the cell compartment of the FTS-20 with specially constructed transfer optics, have been employed.

Many other analytical techniques have been applied in this black carbon research, most of them complementary to the principal tool of FT-IR. The surface and bulk structure of soot have been probed with such spectroscopic methods as Raman, proton NMR, 13C CP/MAS NMR, EPR, ESCA, and mass spectrometry. Elemental analysis, scanning electron microscopy (SEM), thermal analysis, fluorescence, gravimetry, electrochemistry, GC/MS, low temperature N_2 adsorption for surface area, and wet chemical analyses have found application in the structural studies. In addition to FT-IR, microgravimetric, manometric, UV–visible, chemiluminescence, gas filter correlation, and photochemical techniques have been used in the measurements of reaction rates. Details of all of these analytical techniques are found in the referenced articles, and are presented below where needed.

In recent work, the fabrication [26] of a long optical path cell (LOPC) interfaced with the FTS-14B spectrometer and electronically modified Cahn RG microbalance, as well as with a solar simulator (ORC), has made it possible to explore surface changes and heterogeneous reaction rates at p.p.m. concentration levels. Fig. 2 [26] is a diagram of this instrumental system.

2.2. Materials

Soot was collected from a *n*-hexane flame, either on the surface of an infrared-transmitting disc such as CaF_2 or on an inverted funnel, about 50 mm above the flame outlet, and treated by methods previously described (e.g. Ref. [25]). The soot particles are uniformly spheroidal and of about 0.1 μm diameter as determined by SEM. Its surface area is 89 ± 2 m^2 g^{-1} and it has an elemental composition ranging from 87–95% C, 1.2–1.6% H, and 6–11% O. Compressed "zero" air, nitrogen and oxygen were supplied by General Air, and SO_2 and NO_2/N_2O_4 by Matheson.

3. Results and discussion

3.1. Structure

An FT-IR spectrum of *n*-hexane soot, obtained from a 2 mg cm^{-2} sample captured from the flame on a CaF_2 disc, taken in vacuo using the cell illustrated in Fig. 1, is shown in Fig. 3. A second spectrum, Fig. 4, trace 1, is of a sample of the soot in KBr to reveal absorptions below 1200 cm^{-1}. Complex but characteristic absorption bands are apparent at 3040 cm^{-1}, 1800–1700 cm^{-1}, 1630–1560 cm^{-1}, 1440 cm^{-1}, 1260 cm^{-1}, and 900–750 cm^{-1}. A region of high noise above 3200 cm^{-1}, not shown, contains a band due to hydrogen-bonded OH. Each of these absorption

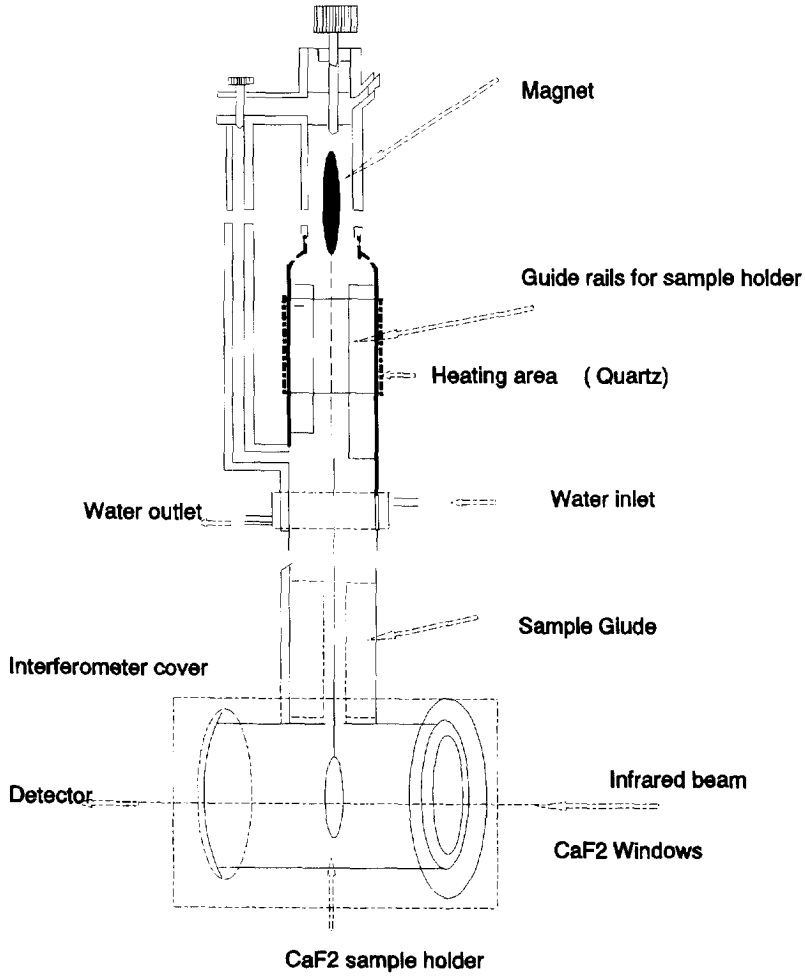

Fig. 1. Vacuum cell for FT-IR measurements. From Akhter et al., Appl. Spectrosc., 39(1) (1985) 143 [25].

bands is observed with every soot sample, but their relative intensities vary with preparation conditions and subsequent treatment. Band assignments were made not only from their frequencies but also from ancillary experiments such as heating, desorption, oxidation, and isotopic substitution, and the effect of these treatments on band position and intensity.

In the 1800–1700 cm^{-1} region three separate bands, at 1775 cm^{-1}, 1740 cm^{-1} and 1720 cm^{-1}, comprise a complex absorption. Thermal desorption experiments, monitored by FT-IR (Fig. 5) and gaseous product analysis [25], revealed that the 1740 cm^{-1} and 1775 cm^{-1} bands change at the same rate on heating and reflect the same species. Decomposition of the functionalities responsible for the 1740 cm^{-1} and 1775 cm^{-1} absorptions is identified with loss of CO_2 and CO during the desorption process. As evident from Fig. 4, trace 2, reoxidation of the thermally treated soot restores these bands, lost during desorption, and confirms from the frequency shifts that they are indeed carbon–oxygen functionalities. The 1740 cm^{-1} and 1775 cm^{-1} bands are identified as the symmetric and asymmetric stretching modes of a cyclic anhydride, while the 1720 cm^{-1} band is from an alkyl carbonyl.

The absorption at 1260 cm^{-1}, from infrared and

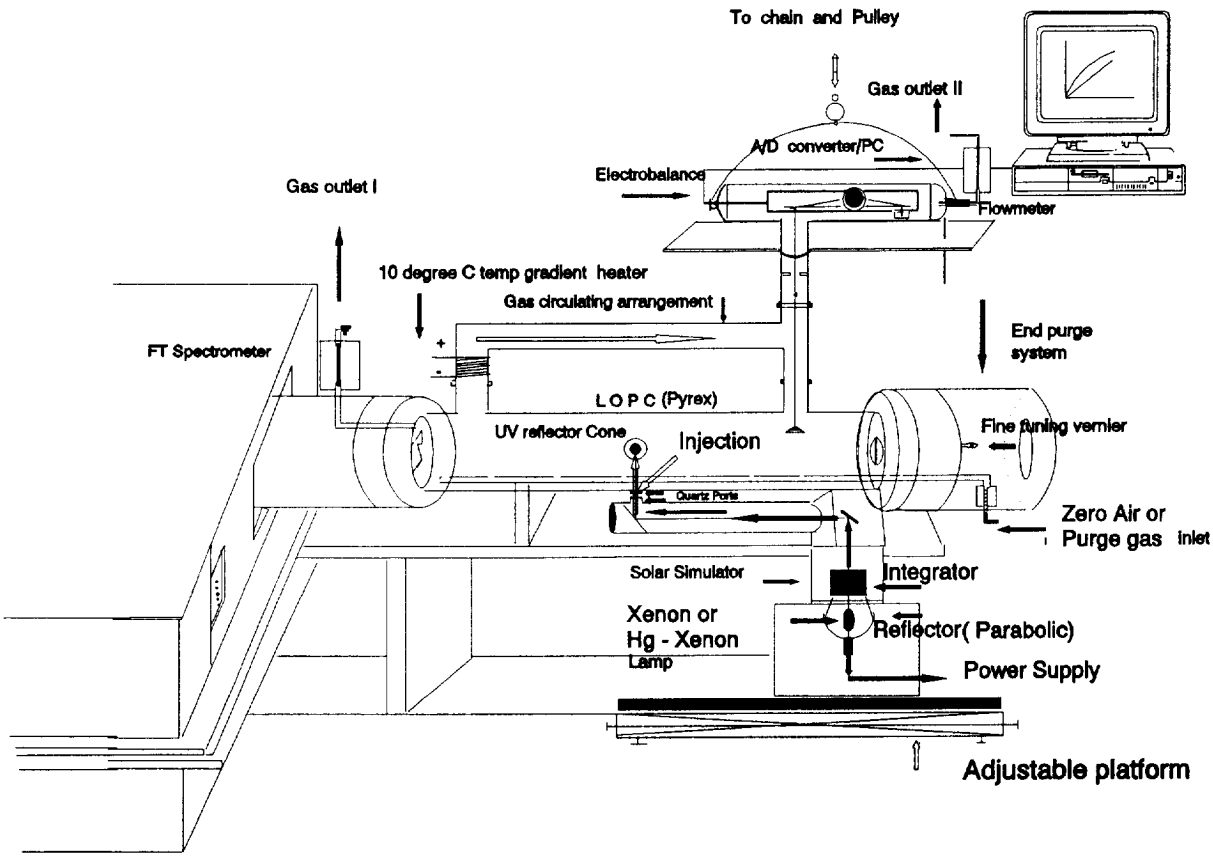

Fig. 2. Long optical path cell interfaced with FT spectrometer and electrobalance.

thermal desorption evidence, has been assigned to C–O–C stretching in the anhydride and an aryl ether linkage. Aryl ethers absorb strongly in the 1210–1310 cm^{-1} region [27], have a tendency to form during pyrolysis and exhibit high stability [28]. Further, a higher-frequency shoulder disappears from the spectrum along with the 1800–1700 cm^{-1} absorption on thermal desorption. Some contribution from =C–H in-plane deformation, although it cannot be identified from these experiments, probably is present as well.

That C–H bonds are present in freshly-prepared *n*-hexane soot was evidenced by absorptions at 3040 cm^{-1}, 1440 cm^{-1}, and in the 900–750 cm^{-1} region. The 3040 cm^{-1} and 1440 cm^{-1} bands always appear together and are most prominent when soot is collected from less-oxidizing flames. Assignment of these to $=CH_2$ would be logical, as would the origin of the 900–750 cm^{-1} bands in out-of-plane C–H deformations of highly substituted aromatics [27]. However, an assignment to oxygen-containing species such as chelated –OH or –carbonyl could not be ruled out in the former case, or peroxy linkages in the latter, without additional experiments. Fig. 4, trace 2 reveals that reoxidation (with $^{18}O_2$) does not restore the 900–750 cm^{-1} bands, as occurs with the carbon–oxygen functionalities. Also, soots from acetone and deuterated acetone (acetone-D_6), and from cyclohexane and C_6D_{12}, were prepared. Table 1 summarizes the results of these deuterium substitutions. Assignments of the 3040 cm^{-1} and 1440 cm^{-1} bands to unsaturated C–H, and of the 880 cm^{-1}, 840 cm^{-1} and 760 cm^{-1} bands to aromatic C–H with 1,2,4- and 1,3-substitution, respectively, have been made [29].

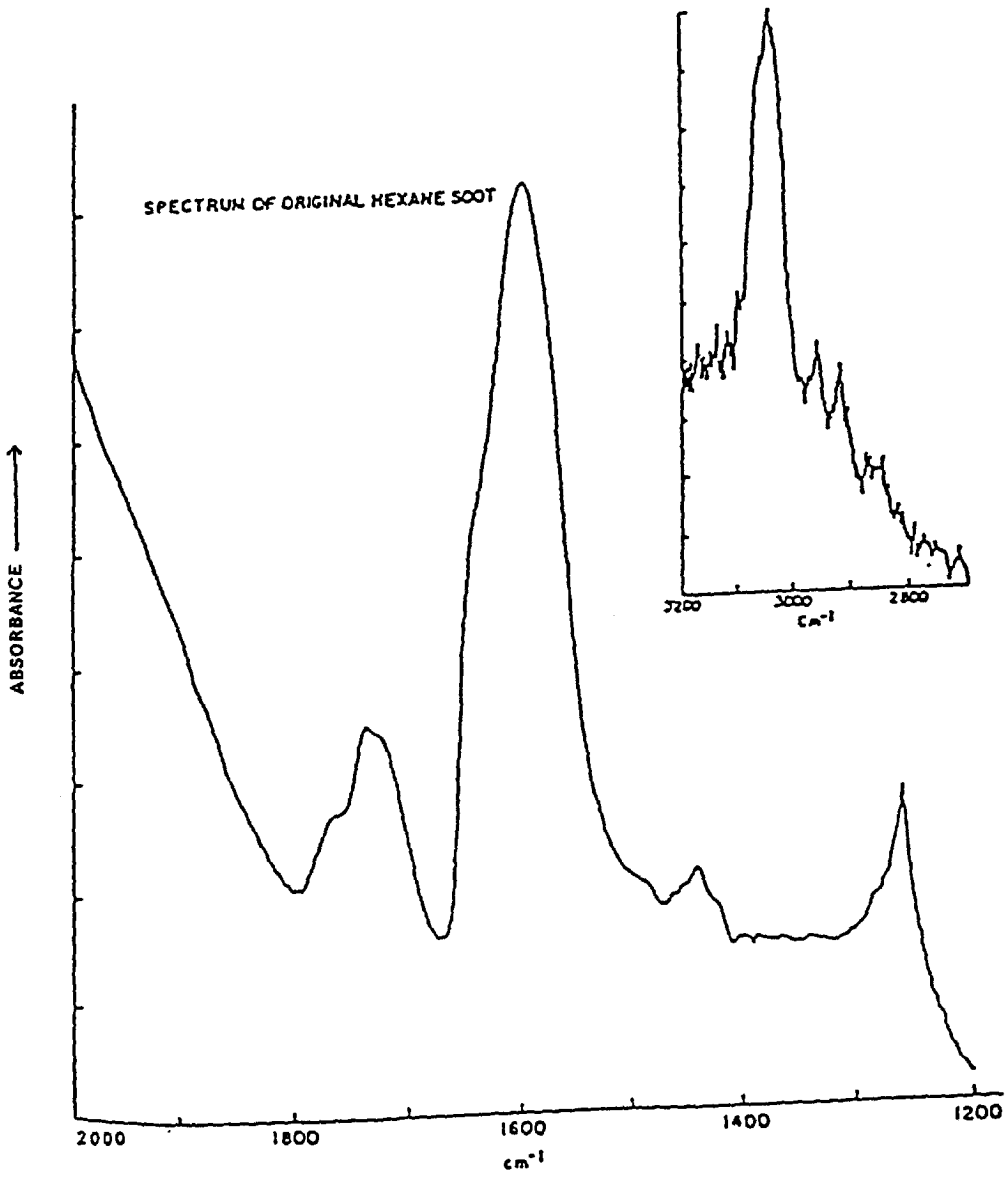

Fig. 3. FTIR spectrum of *n*-hexane soot. From Akhter et al., Appl. Spectrosc., 39(1) (1985) 143 [25].

A strong and persistent infrared absorption at 1590 cm^{-1} is the dominant and most characteristic one in all carbons, chars, coals, soots, etc. Its origin has been speculated upon by nearly every investigator to study the infrared spectra of carbons in the last 50 years (see Refs. e.g. [9–19,30–48]). Among the most common assignments for this band are chelated carbonyl or the C=C stretching modes of an aromatic system, neither of which can explain the full range of data obtained in our work. Combining thermal desorption with reoxidation of soot by $^{16}O_2$ and $^{18}O_2$, monitored by FT-IR, has provided an unambiguous interpretation of the 1590 cm^{-1} band of hexane soot which presumably is applicable to other black carbons. Fig. 6, trace B shows the enhancement of the 1590 cm^{-1} band

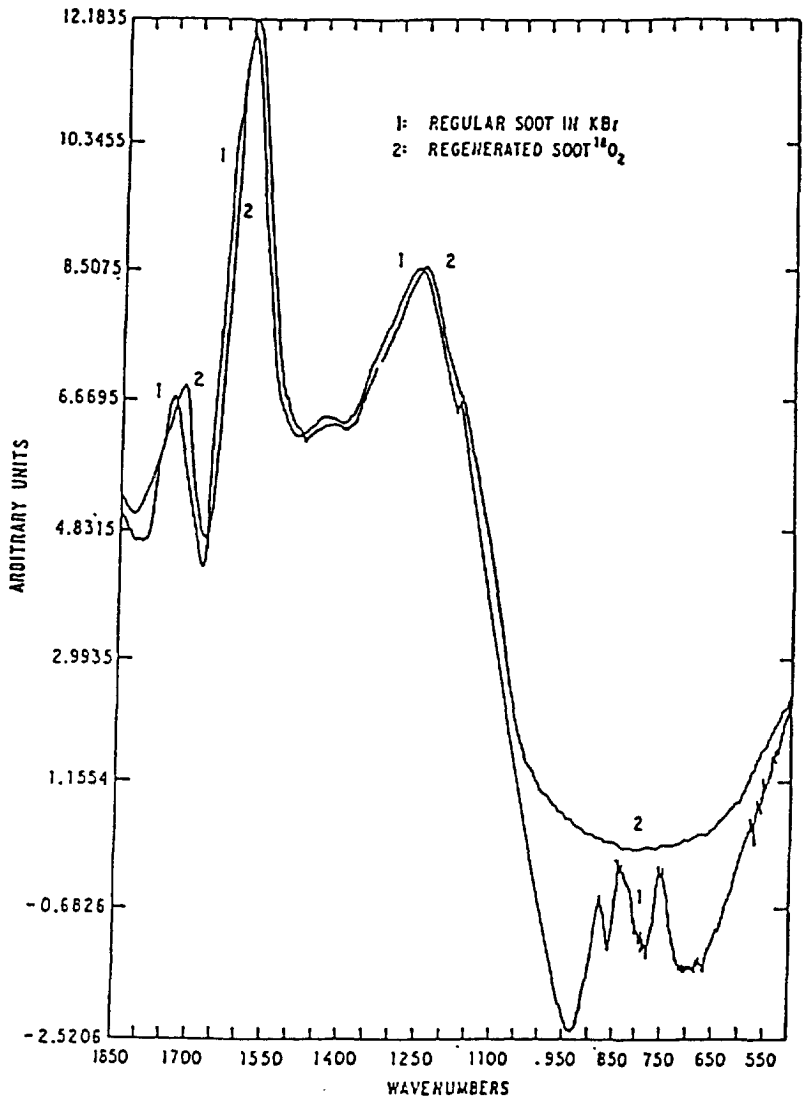

Fig. 4. Spectra of *n*-hexane soot in KBr. From Jassim et al. Appl. Spectrosc., 40 (1986) 113 [29].

upon $^{16}O_2$ reoxidation of soot which has been heated to 600°C, revealing that neither oxygen functionalities nor aromaticity alone can be responsible for this absorption. Reoxidation with $^{18}O_2$, the experiments shown in Fig. 7, trace B also results in the disappearance of a shoulder at about 1630 cm^{-1} which is always present in the original soot. Coupling these experiments with the observations [49,50] that a carbonyl conjugated with an aromatic system can have its frequency lowered to the 1600 cm^{-1} region, while significantly enhancing the intensity of the aromatic stretching absorption in the same frequency range, provides the answer. The characteristic 1590 cm^{-1} band in the black carbons is due to the aromatic stretching enhanced by its conjugation with carbonyl, itself lowered in absorption frequency to the same region.

Evaluations of soot by spectroscopic methods other than FT-IR have explored aspects of the bulk structure such as aromaticity. For example, 13C CP/MAS NMR and FT-IR spectra have yielded estimates [25] of aromaticity, *fa*, of hexane

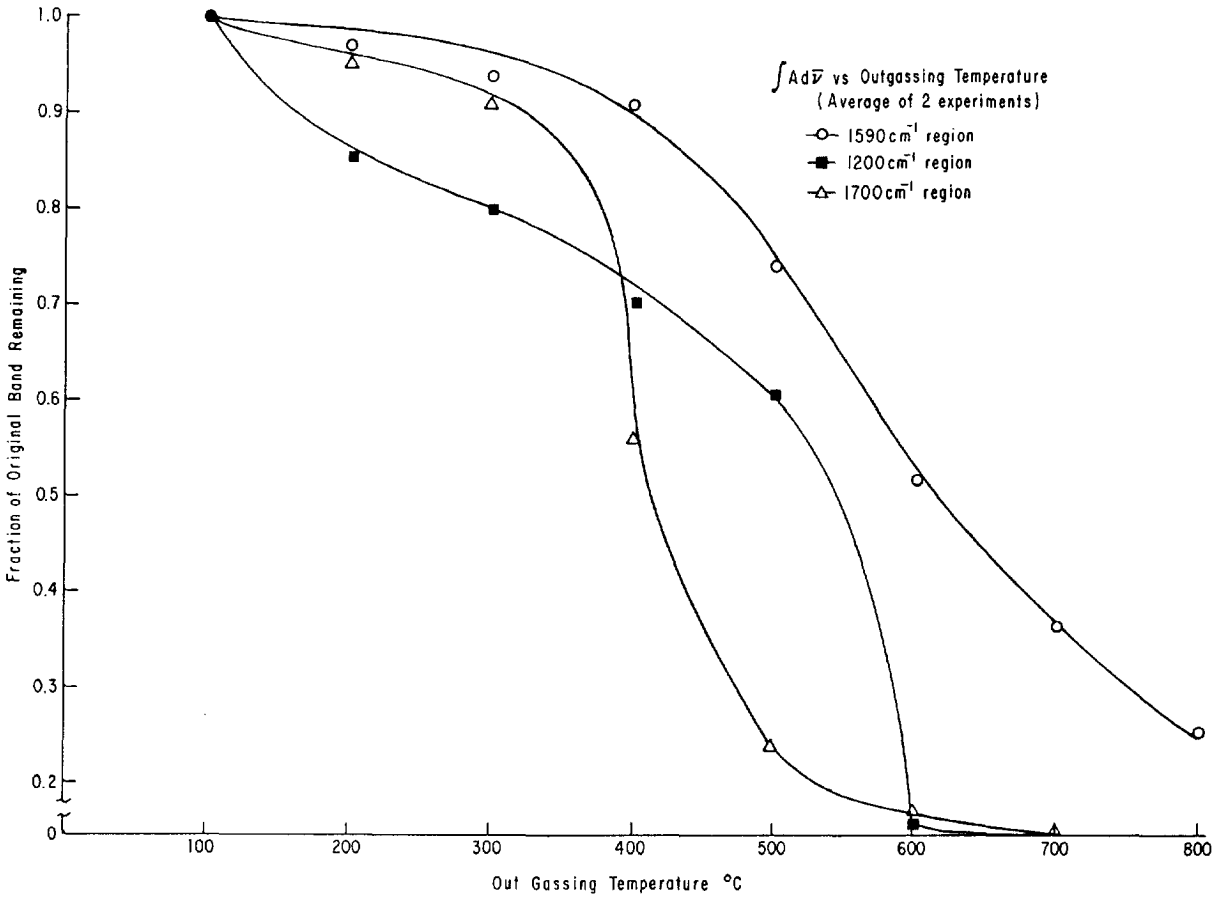

Fig. 5. Integrated absorbance vs. desorption temperature. From Akhter et al., Appl. Spectrosc., 39(1) (1985) 143 [25].

Table 1
Comparison of absorption frequencies involving H for regular and deuterated soots

Soot origin	Frequency (cm^{-1})						
n-Hexane	3550[a]	3040	1440	887	840	775	
Acetone	3480	3090	1440	880	840	760	
Acetone-D6	3340	2260	1330	832	738	592	540
Cyclohexane	3550[a]	3040	1440	–[b]	–	–	
Cyclohexane-D12	X	2268	X	–	–	–	

[a] Bands broad and weak. [b] Spectra not acquired. X No bands discernible.

soot

$$fa = C_{arc}/C_{ali} = 0.9 \quad (2)$$

which is within the range of coal and related highly aromatic materials [51]. This conclusion is confirmed by its EPR spectrum, which consists of a single symmetrical line with a width of 3.25 gauss devoid of hyperfine structure, and having a *g* value of 2.0058. These parameters also are consistent with values for coal and other graphitic materials [52–54].

Further structural details were explored [55] with a sequential solvent extraction scheme using a suite of solvents of increasing polarity from *n*-hexane to acetonitrile. Successive extracts were analyzed by FT-IR, UV–visible, fluorescence, and NMR spectroscopies, as well as by GC/MS. Cumulative solvent extraction removed one third of the total soot mass and SEM measurements showed the particle diameter to increase by 20%, the latter undoubtedly due to the replacement of

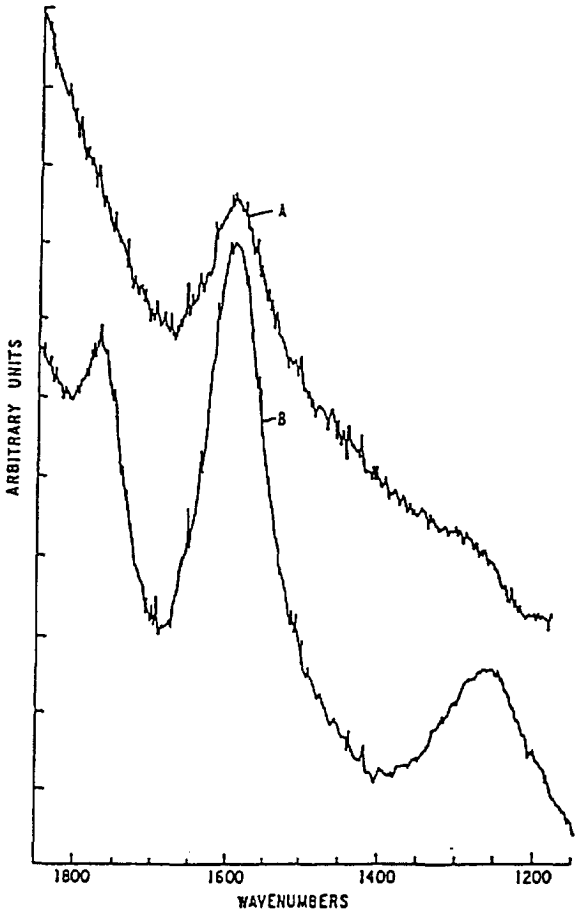

Fig. 6. FT-IR spectra of *n*-hexane soot; (trace A) degassed for 2 h at 600°C, (trace B) reoxidized after 800°C degassing (1 h) with 100 torr $^{16}O_2$. From Akhter et al., Appl. Spectrosc., 39(1) (1985) 143 [25].

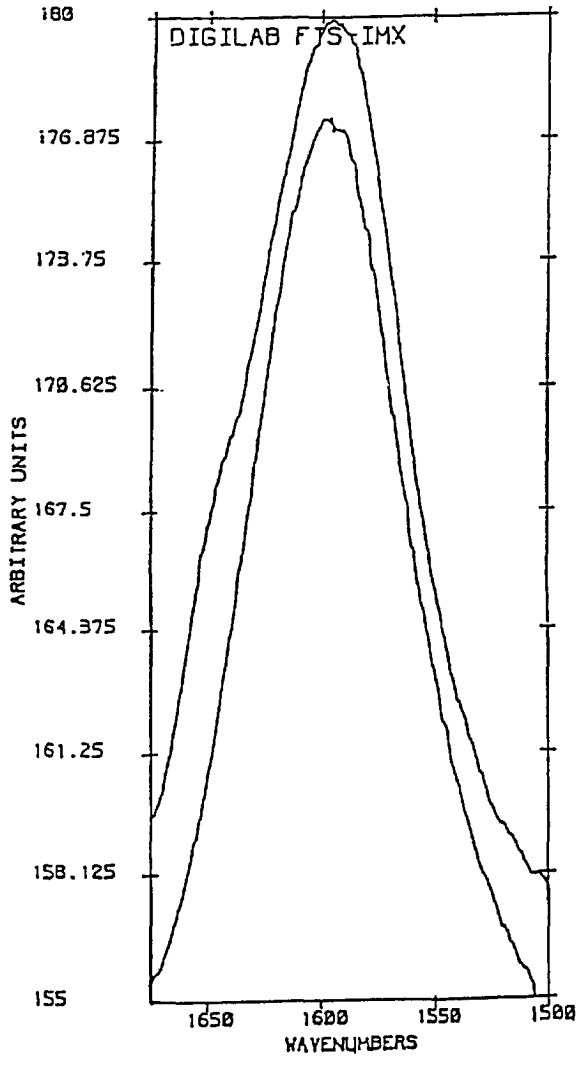

Fig. 7. Superimposed spectra of *n*-hexane soot; (trace A) evacuated at 10^{-6} torr at 22°C for 4 h, (trace B) outgassed at 800°C, reoxidized with 100 torr $^{18}O_2$ at 360°C for 12 h, then evacuated at 10^{-6} torr. Adapted from M.S. Akhter, J.R. Keifer, A.R. Chughtai and D.M. Smith, Carbon, 23 (1985) 589–591.

extracted moieties by solvent. The principal conclusions reached by these extraction experiments were:

(i) Significant among the components of *n*-hexane soot are polyaromatic hydrocarbons (PACs) and oxygenated polyaromatics (O-PACs). Although distinguishing among some of the enormous number of isomers of these compounds was not possible, examples of the species found are illustrated in Fig. 8.

(ii) Characteristic functionalities which are observed by direct infrared examination of the soot (Fig. 3) also are on the nonextractable portion, or "backbone" of the soot particle, as revealed by Fig. 9.

Thus, the detailed study of *n*-hexane soot utilizing several analytical techniques, but with FT-IR spectroscopy as the principal and most definitive tool, has led to conclusions regarding the structure of soot and related materials. Integration of all data yields a picture of a typical segment as represented in Fig. 10 [55], and the 3-dimensional representation shown in Fig. 11 [24]. While the latter appears graphitic in nature,

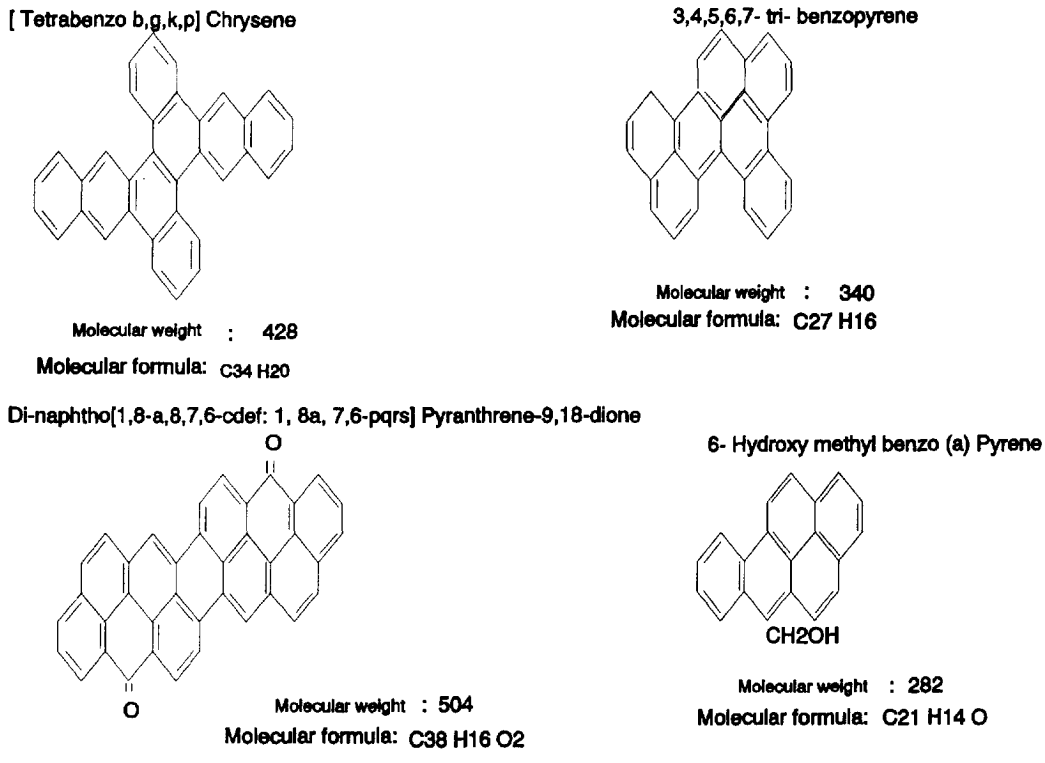

Fig. 8. Some solvent-extracted components of *n*-hexane soot.

the physical properties and other studies [56] of soot suggest that the aromatic layers are held together by as yet undefined carbon structures which are more reactive than the aromatic systems themselves.

3.2. Reactivity

The role of black carbon as a reactant or catalyst in heterogeneous reactions involving pollutant species, especially oxidants, in the troposphere is a question prompted by its atmospheric concentrations. Because of the definitive character of FT-IR in identifying surface functional groups, and its adaptability to their quantitative estimation as a function of time, it was the analytical method of choice for many of the carbon surface reaction rate measurements.

3.2.1. Oxides of nitrogen

Since fossil fuel combustion is a principal source of oxides of nitrogen in the atmosphere, and because they are contributors to the formation of photochemical smog, their reactions with black carbon have been studied extensively in these laboratories. The kinetics of these reactions have been determined over a wide range of pressures, temperatures, and concentrations of other species such as water vapor and oxygen.

Fig. 12 [57] shows the FT-IR subtraction spectra of *n*-hexane soot after contact with NO_2/N_2O_4 (60 torr, 22°C, followed by evacuation to 10^{-5} torr) as a function of contact time. The absorption bands at 1660 cm^{-1}, 1540 cm^{-1}, 1400 cm^{-1}, 1340 cm^{-1}, 1305 cm^{-1}, and 1280 cm^{-1} are from new species formed at the carbon surface by reaction with NO_2/N_2O_4. Qualitative identification of the species giving rise to these bands was through the extensive literature on characteristic frequencies in this spectral region, their rates of change, and through reactions with isotopically substituted NO_2 in the form of $^{15}NO_2$ and $N^{18}O_2$. Fig. 13 [57] compares the FT-IR subtraction spectra of soot reacted with NO_2 with one after

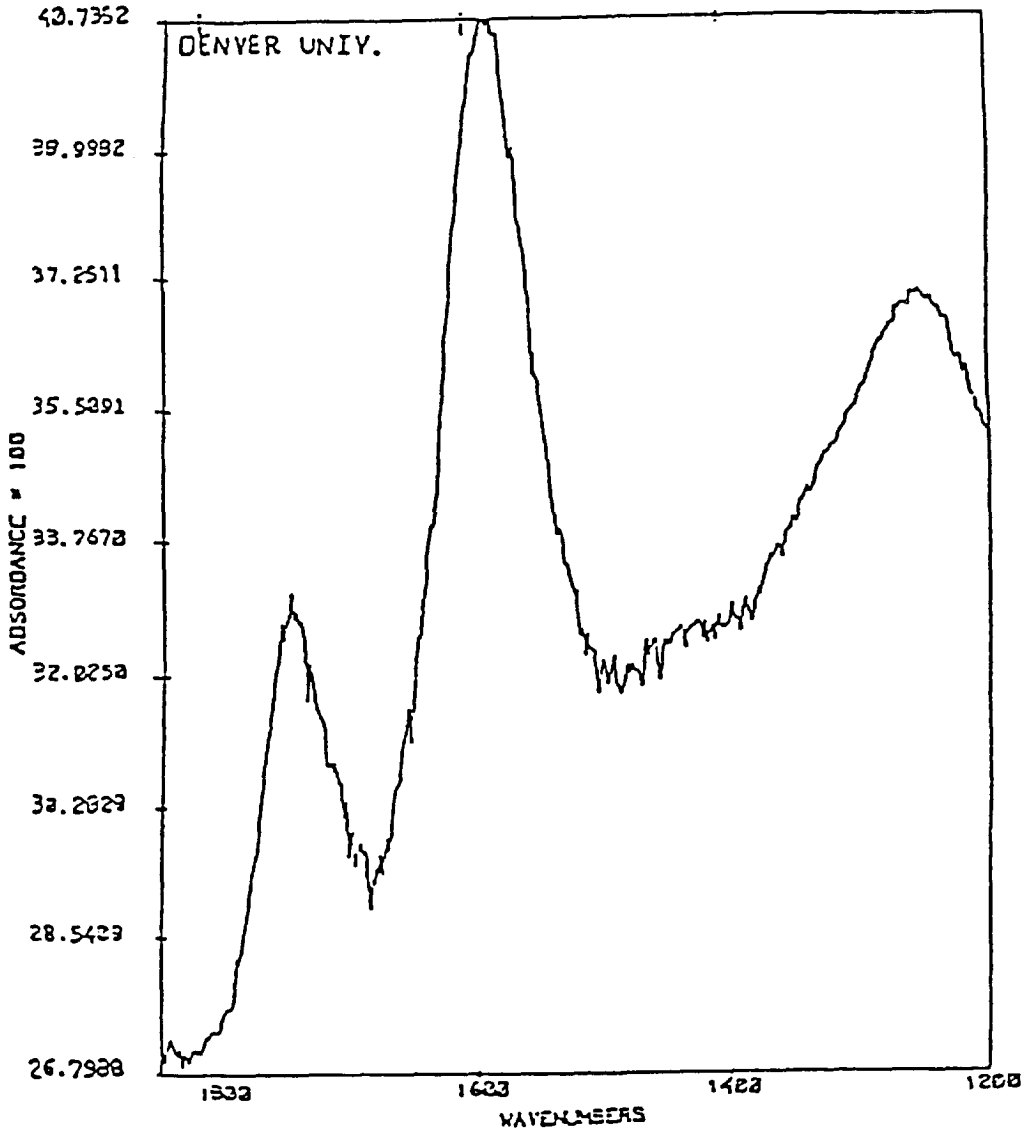

Fig. 9. FT-IR spectrum of residual soot, following extraction with a suite of solvents, dried in vacuum oven at 90°C for 24 h; in KBr with KBr reference. From Akhter et al., Appl. Spectrosc., 39(1) (1985) 154 [55].

reaction with $^{15}NO_2$ under the same experimental conditions (30 torr NO_2 contact, 22°C, $P = 10^{-5}$ torr). Isotopic shifts of all bands, except those at 1775 cm^{-1}, 1730 cm^{-1} and 1400 cm^{-1}, are observed. The absorption frequencies, isotopic shifts, calculated (harmonic oscillator) values, and assignments are summarized in Table 2. Assignments of the bands at 1540 cm^{-1} and 1340 cm^{-1}, 1565 cm^{-1} and 1305 cm^{-1}, and 1660 cm^{-1} and 1280 cm^{-1} to R–NO_2, R–N–NO_2 and R–O–N=O, respectively, are further supported by simultaneous variations in intensity with reactant concentration and time. Experiments with $N^{18}O_2$ confirm that the absorptions at 1775 cm^{-1} and 1730 cm^{-1}, unshifted by reaction with $^{15}NO_2$, are due to carbon–oxygen vibrations of new lactones or alkyl carbonyls. These experiments also demonstrated that the NO_2/N_2O_4 reactant was

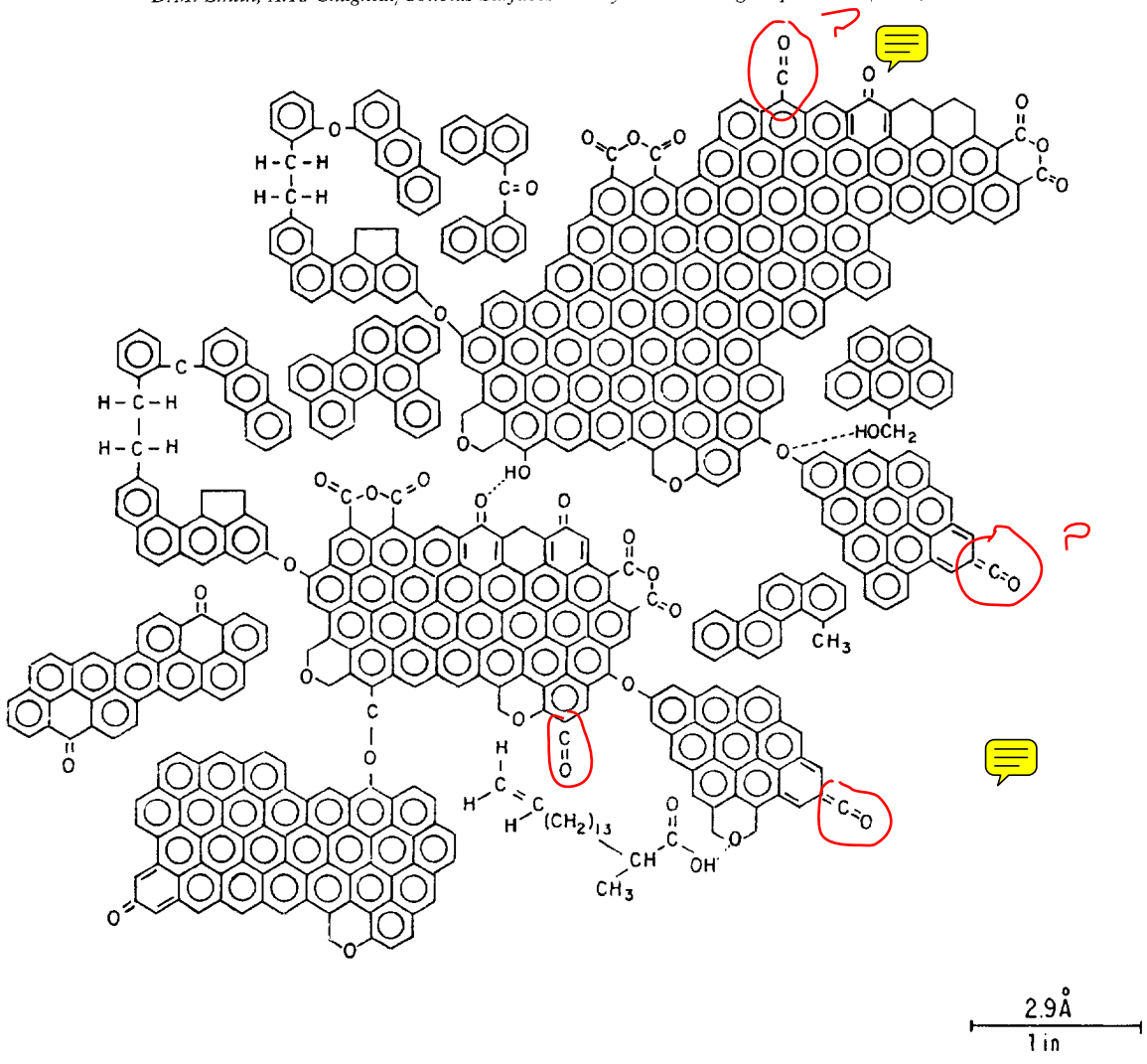

Fig. 10. Representation of hexane soot segment as formed in the flame. From Akhter et al., Appl. Spectrosc., 39(1) (1985) 154 [55].

the origin of the oxygen atoms of all new functionalities. The small 1400 cm^{-1} band, assigned to new OH deformation, indicates that some OH is created by reaction of carbon surface groups with NO_2/N_2O_4.

While Fig. 12 illustrates the increase in surface species with time at a constant NO_2 pressure, Fig. 14 shows the dependence of rate on P_{NO_2}. The latter, a plot of integrated absorbance ($\int A(\nu)\,d\nu$) vs. time, indicates a depletive chemisorption process. Accordingly, the data were analysed utilizing the Elovich equation [58]; this model for such processes may be expressed as:

$$dq/dt = a \exp(-\alpha q) \quad (3)$$

where q is the amount of adsorbate, α is a constant, characteristic of the process, and a is the initial reaction rate.

The integrated form of the equation

$$q = (2.3/\alpha)[\log(t + t_0)] - (2.3/\alpha)[\log t_0] \quad (4)$$

where $t_0 = 1/\alpha a$, may be used to determine the initial rate of the reaction. Selection of a t_0 value by computer to yield a linear plot, as illustrated in

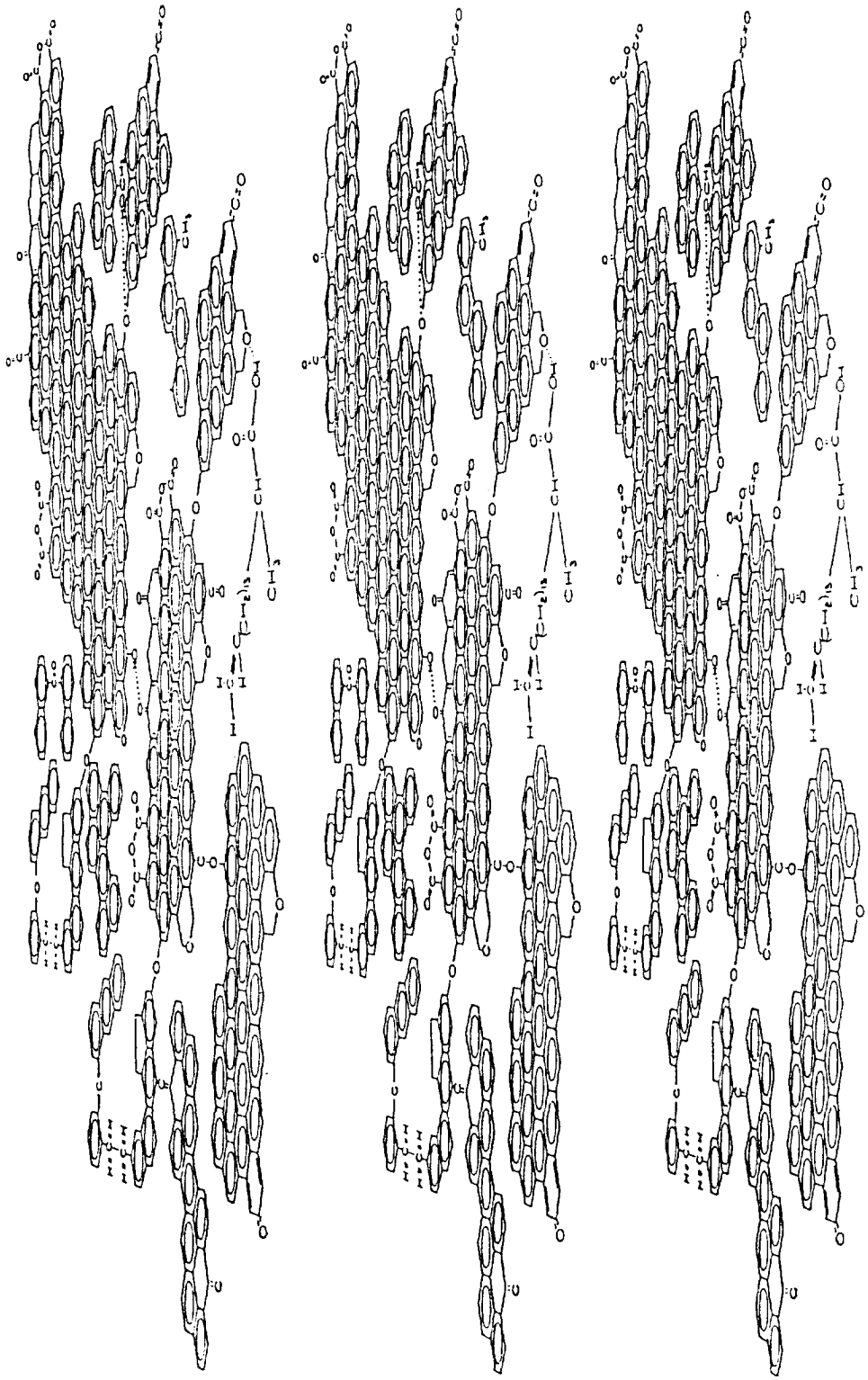

Fig. 11. Three-dimensional model of *n*-hexane soot. From Sergides et al., Appl. Spectrosc., 41(3) (1987) 482 [56].

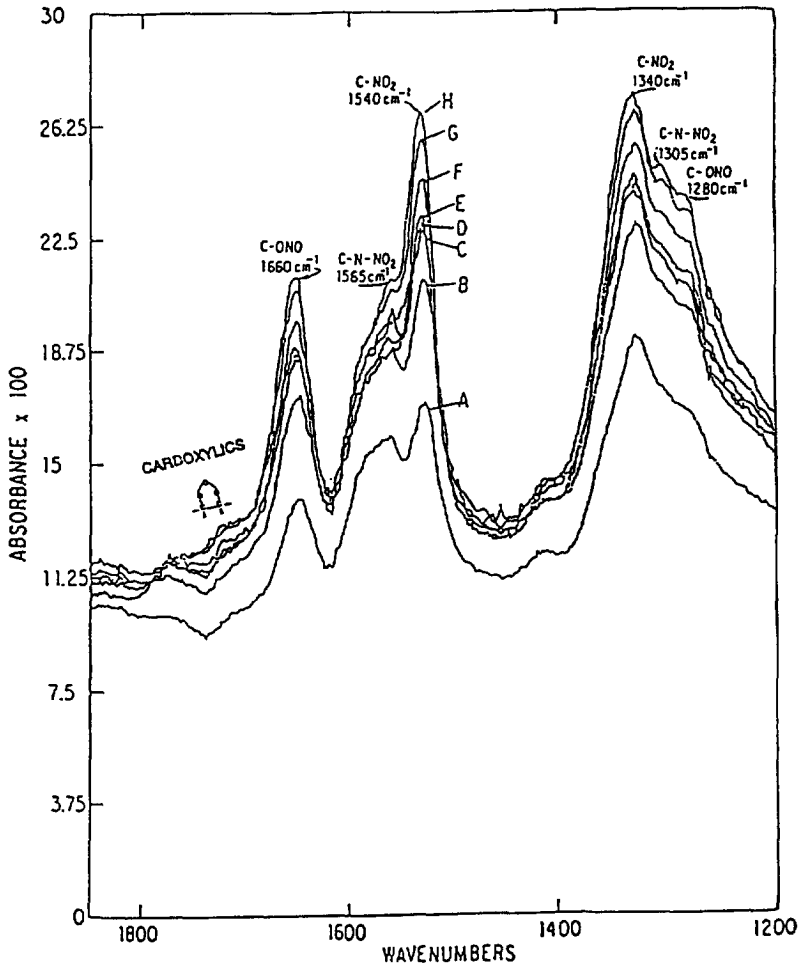

Fig. 12. Soot spectrum subtracted from that of soot contacted with NO_2 (60 torr, 22°C). (trace A) 1 min, (trace B) 2 min, (trace C) 3 min, (trace D) 4 min, (trace E) 5 min, (trace F) 10 min, (trace G) 20 min, (trace H) 45 min. From Akhter et al., J. Phys. Chem., 88 (1984) 5334 [57].

Fig. 15, enables the calculations of α from the slope. As revealed by Fig. 16, the formation rates of both the 1660 cm^{-1} and 1540 cm^{-1} absorption bands, from the R–O–N=O and R–NO_2 species, have a first-order dependence on NO_2. The rate law thus determined from these spectroscopic measurements is, for example,

$$d[CNO_2]/dt = k_1 P_{NO_2} + k_2 = k P_{N_2O_4}^{\frac{1}{2}} + k' \qquad (5)$$

indicating a dual path mechanism. This series of experiments, at relatively high NO_2/N_2O_4 pressures, was not applicable to determining the rate dependence on soot.

The development of the LOPC [26] and its interfaces with FT-IR spectrometer, microbalance and solar simulator, illustrated in Fig. 2, has made it possible not only to study this reaction at much lower NO_2/N_2O_4 pressures (9–35 p.p.m.) but also to determine its dependence on soot. Figs. 17 and 18 show both the NO_2 and soot dependences of reaction rate, determined microgravimetrically in this case [59], but consistent with spectroscopic results at higher pressures. The rate expression for this soot surface reaction in the p.p.m. NO_2 range is:

$$\text{Initial rate} = (k_1 + k_2\,[\text{soot}]^{\frac{1}{2}}) P_{NO_2} \qquad (6)$$

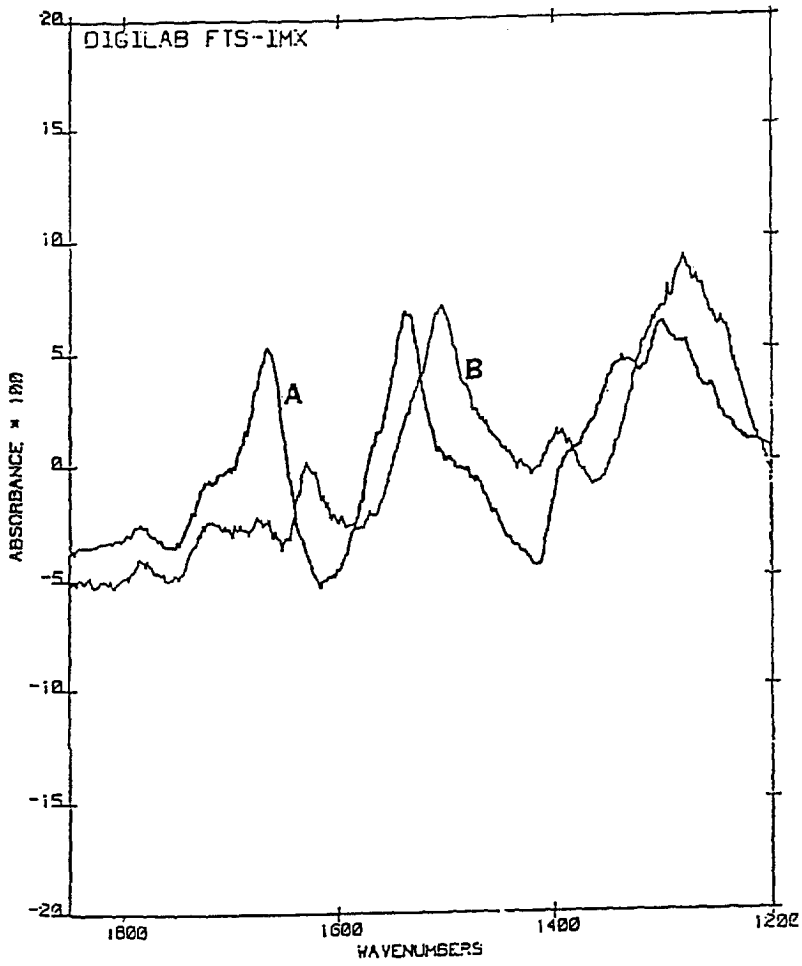

Fig. 13. FT-IR subtraction spectra of *n*-hexane soot contacted with NO_2: (trace A) $^{14}NO_2$ (30 torr, 22°C), $P = 10^{-5}$ torr; (trace B) $^{15}NO_2$ (30 torr), $P = 10^{-5}$ torr. From Akhter et al., J. Phys. Chem., 88 (1984) 5334 [57].

also indicating a dual path mechanism. Such a mechanism consistent with the data is:

Path 1

$N_2O_4 \underset{k_{-1}}{\overset{k_1}{\rightleftharpoons}} 2NO_2$ Fast equilibrium {1}

$C_{surf} + NO_2 \xrightarrow{k_2} C\text{–}NO_2$ Rate determining {2}

$C_{surf} + NO_2 \xrightarrow{k_3} C\text{–}ONO$ Rate determining {3}

Path 2

$C_{surf} + NO_2 \underset{k_{-4}}{\overset{k_4}{\rightleftharpoons}} C_{surf}{\cdot}NO_2$ Fast {4}

$C_{surf}{\cdot}NO_2 \xrightarrow{k_5} C\text{–}NO_2$ Rate determining {5}

and/or

$C_{surf}{\cdot}NO_2 \xrightarrow{k_6} C\text{–}ONO$ Rate determining {6}

Table 2
Products of the soot–NO_2/N_2O_4 reaction

Absorption (cm^{-1})	$^{15}NO_2$ (cm^{-1})	$-\Delta\nu$, (cm^{-1})	Calculated[a]	Assignment
1775	1775	0		(Lactone and/or alkyl carbonyl)[b]
1730	1730	0		
1660	1630	30	37	R–O–N = O(chelated)[c]
1565	1540	25	32	R–N–NO_2
1540	1505	35	39	R–NO_2
1400	1400	0		–OH (deformation)
1340	1310	30	34	R–NO_2
1305	1285	20	27	R–N–NO_2
1280	1250	30	29	R–O

[a] Calculated from harmonic oscillator model.
[b] Consistent with $N^{18}O_2$ experiments.
[c] Nonchelated R–O–N = O assumed beneath 1600 cm^{-1} region.

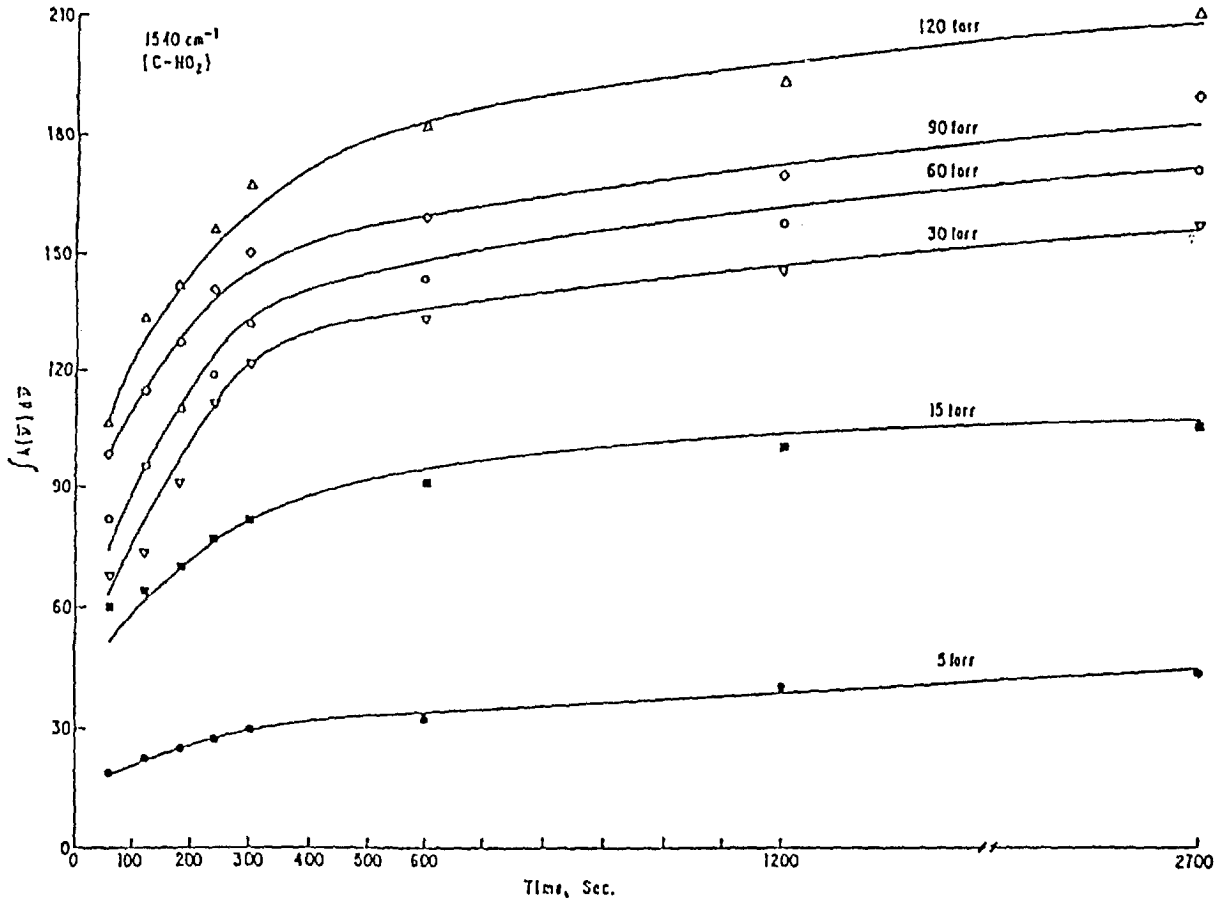

Fig. 14. Integrated absorbance of the 1540 cm^{-1} (C–NO_2) band formed on soot as a function of time at various NO_2 pressures. From Akhter et al., J. Phys. Chem., 88 (1984) 5334 [57].

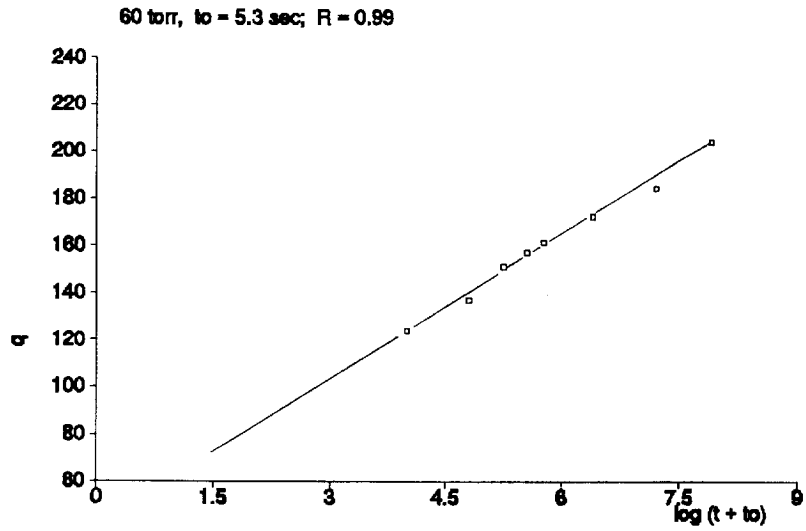

Fig. 15. Elovich plot for 1660 cm^{-1} band (C–ONO) in NO_2 soot system (60 torr, 22°C). From Akhter et al., J. Phys. Chem., 88 (1984) 5334 [57].

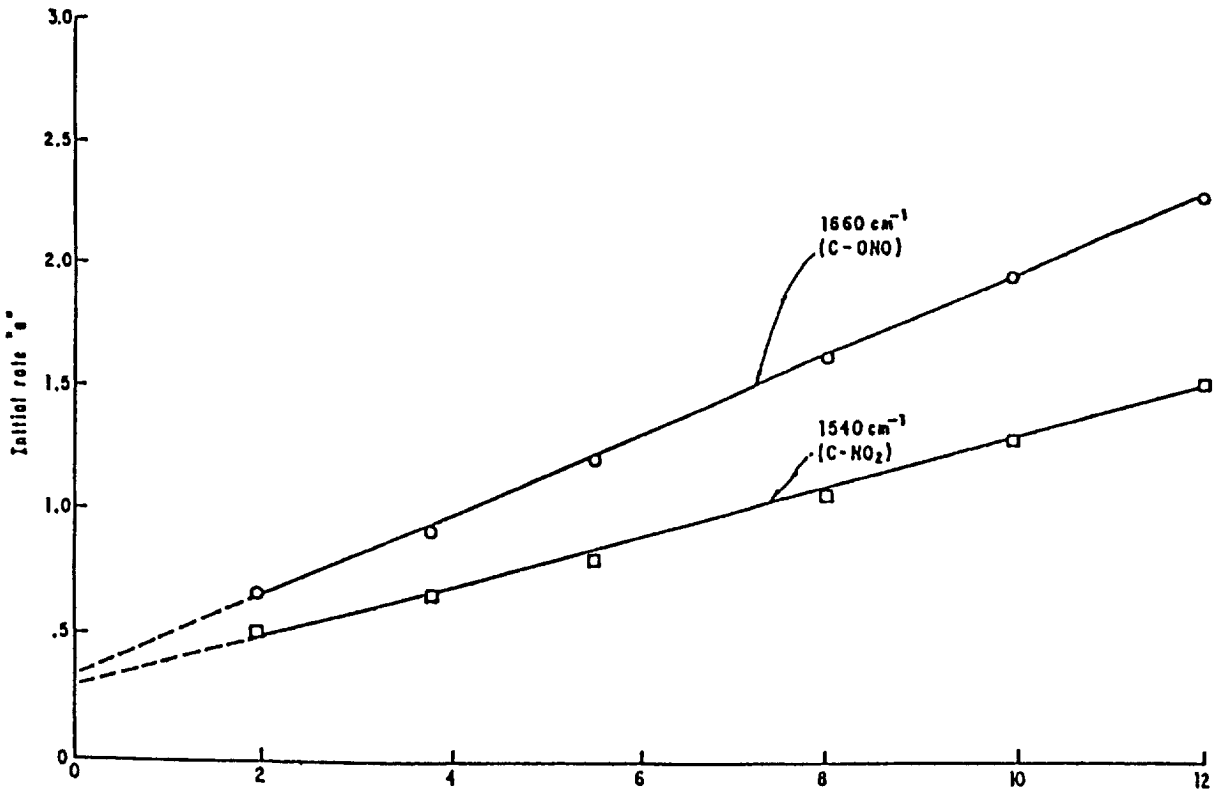

Fig. 16. Dependence of initial rate on partial pressure of NO_2 in the NO_2/soot system at 22°C. From Akhter et al. J. Phys. Chem., 88 (1984) 5334 [57].

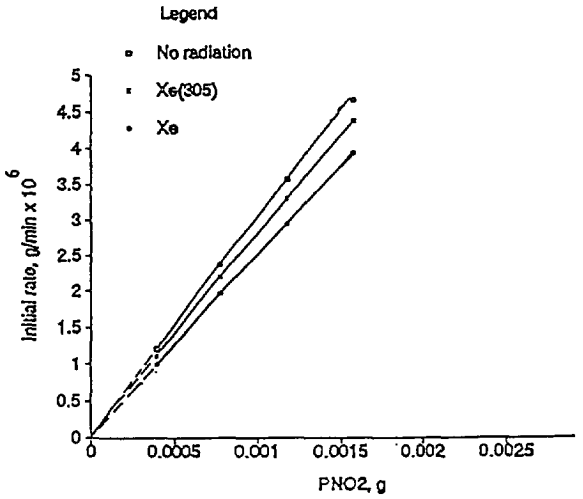

Fig. 17. Initial rate of the soot–NO_2/N_2O_4 reaction as a function of NO_2 concentration with and without simulated solar radiation. From Chughtai et al., Carbon, 32(2) (1994) 405 [59].

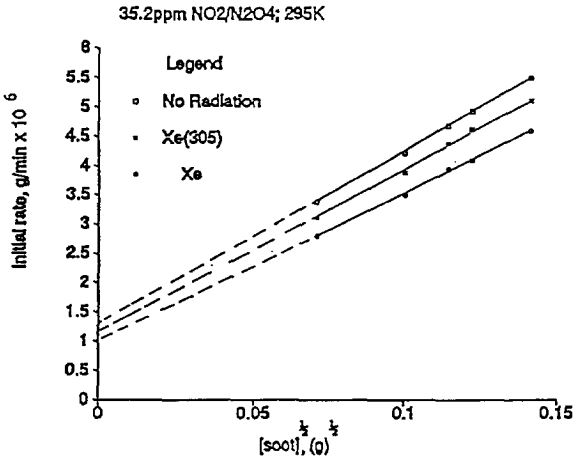

Fig. 18. Initial rate of the soot-NO_2/N_2O_4 reaction as a function of soot with and without simulated solar radiation. From Chughtai et al., Carbon, 32(2) (1994) 405 [59].

or

$$2C_{surf} + N_2O_4 \underset{k_7}{\overset{k_7}{\rightleftharpoons}} C_2{\cdot}N_2O_4 \qquad \text{Fast } \{7\}$$

$$C{\cdot}\tfrac{1}{2}N_2O_4 \xrightarrow{k_8} C{-}NO_2 \qquad \text{Rate determining } \{8\}$$

and/or

$$C{\cdot}\tfrac{1}{2}N_2O_4 \xrightarrow{k_9} C{-}ONO \qquad \text{Rate determining } \{9\}$$

Rate law

$$\text{Rate} = (k + k_3)\{C^*_{surf}\}[NO_2] + (k_5 + k_6)\{C^T_{surf}\}[NO_2]/((k_4 + k_5 + k_6)/k_4) + [NO_2]) \qquad (7)$$

Experimental rate law

$$\text{Initial rate} = (k + k'\{\text{soot}\}^{\frac{1}{2}})[NO_2] \qquad (6)$$

(At high P_{NO_2}, Eq. (6) adopts the form of Eq. (5)).

An additional feature of this reaction, revealed by irradiation with the solar simulator is shown in Figs. 17 and 18. A decrease of 5–15% in the apparent rate constants (k_1 and k_2) of Eq. (6) is observed in going from ordinary light to a Xe lamp filtered to 50% intensity at 305 nm to an unfiltered lamp. The phenomenon is explained solely by the photolytic dissociation of NO_2 at wavelengths below 420 nm [60]

$$NO_2 + h\nu(\lambda \leqslant 420\text{nm}) \rightarrow NO + O \qquad (8)$$

as revealed by data illustrated in Fig. 19. The decrease in reactant concentration at the soot

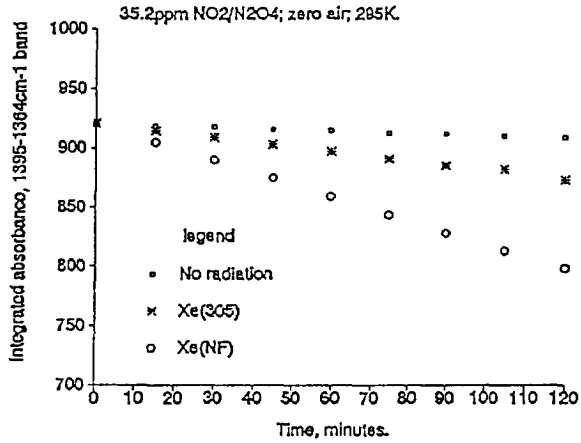

Fig. 19. Rate of decrease of NO_2 in the absence of soot. From Chughtai et al., Carbon, 32(2) (1994) 405 [59].

surface, being replaced by the unreactive species NO [61,62] and apparently ^3P oxygen atoms, is responsible for the decreased rate.

Infrared spectroscopy also has proven to be a valuable tool in studies of the soot-oxides of nitrogen reactions under varying conditions of temperature, pressure and concentrations of the reactant species. For example, in a study [63] of the soot and NO_2/N_2O_4 reaction at higher concentrations above 60°C a *major redox reaction* was discovered. This reaction is rapid and accompanied by the evolution of large quantities of NO, N_2O, CO, CO_2 concomitant with loss of the bulk (82–95%) of soot. The reaction is second order in NO_2 concentration and zero order in the amount of soot, obeying the rate law

$$dCO_2/dt = k[NO_2]^2\{Soot\}^0 = (k/K_p)\,[N_2O_4]\,\{Soot\}^0 \quad (9)$$

where

$$K_p = [N_2O_4]/[NO_2]^2 \quad (10)$$

Fig. 20, the FT-IR spectrum of a sample of soot following a period of this major redox reaction, reveals all the spectroscopic features of the results of reactions at lower concentrations and temperature except for a sharp stable absorption at 1390 cm^{-1}. Following heating overnight at 87°C, that band is removed; we attribute it to a *complex intermediate* through which the reaction proceeds. This surprising reaction can be explained by the high concentration of unpaired electrons in the soot [64] and the increased fraction of NO_2 monomer present at elevated temperatures. The mechanism, then, is believed [63] to be:

Higher NO_2/N_2O_4 concentration

$$3C\,(s) + 4NO_2\,(g) \rightarrow [C_3(NO_2)_4]^* \rightarrow 3CO_2 + 2N_2O \quad (11)$$

Lower NO_2/N_2O_4 concentration

$$C(s) + NO_2\,(g) \rightarrow [C{\cdot}NO_2]^* \rightarrow CO + NO \quad (12)$$

where the stoichiometry of the intermediate

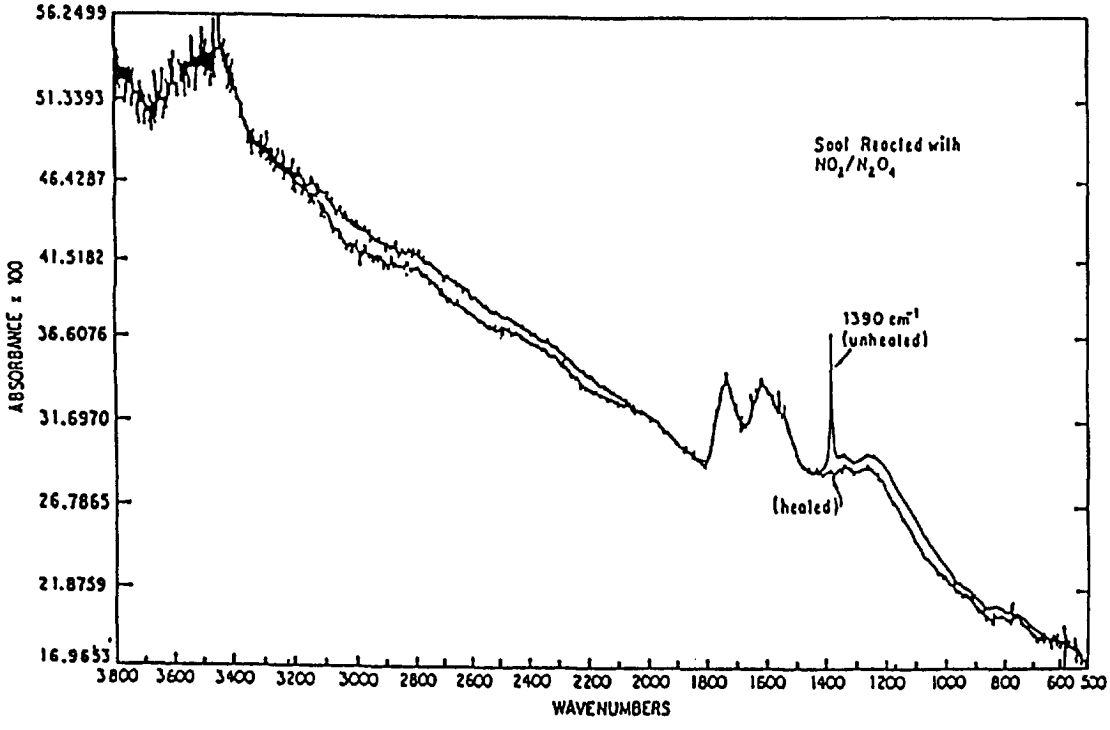

Fig. 20. FT-IR spectra of soot before and after heating samples from the major redox reaction. From Chughtai et al., [63]. Carbon, 28 (2/3) (1990) 411.

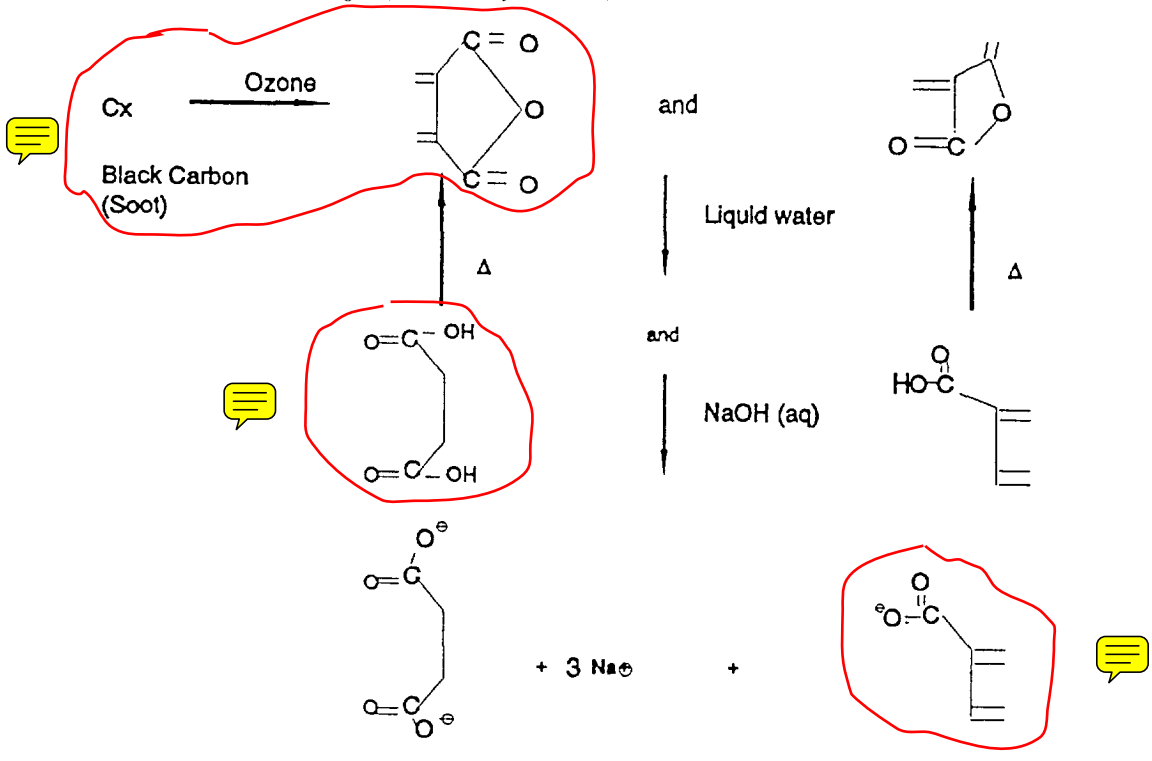

depends upon the concentration of gas-phase NO_2 at the surface. These mechanisms also are consistent with the FT-IR study of gaseous products carried out during this work.

3.2.2. Ozone

Ozone is found in polluted atmospheres and, as a strong oxidant, is reactive toward carbonaceous materials. Accordingly, it is one of those species being given substantial attention in our research program. Generated through the effect of solar radiation on reactions of oxides of nitrogen, oxygen and hydrocarbons, ozone is found at the earth's surface at concentrations normally in the range 0.01–0.07 p.p.m., but occasionally reaching 0.1–0.5 p.p.m. in local environments [65]. Qualitative and quantitative studies of the reaction of O_3 with *n*-hexane soot, over a wide range of experimental conditions, have yielded kinetics and mechanisms as well as structural insights about black carbon. One of the more important reactions is the rapid formation of carboxylic groups on the soot surface. Fig. 21 [66] is FT-IR spectra of this reaction occurring at 22°C, in 1.5% O_3/O_2, with time. This reaction underlies a remarkable solubility of soot particles in aqueous systems, which proceeds by a mechanism demonstrated through a sequence of chemical and infrared measurements [66].

A decrease in pH with mass of soot in aqueous solution, first of all, suggested surface carboxylic acid dissociation as the origin of the "solubilization" phenomenon. Subsequent FT-IR spectra of the soluble and insoluble fractions of soot, of soot solubilized in NaOH solution, and of the effects of heating on the separated solids have confirmed the following mechanism as responsible for the solubilizing effect of ozone on soot in an aqueous environment.

Since theoretical calculations [66] showed that the upper time limit for soot solubilization, in the presence of 20–80 p.p.b.v. ozone, is of the order of a few min, spectroscopic and solubility measurements were carried out on Denver, CO ambient air particulate samples containing black carbon. Fig. 22 and 23 illustrate the results. As the air mass moves through the Denver region from southwest to northeast, Englewood to Welby, the longer tropospheric-residence time is reflected in higher

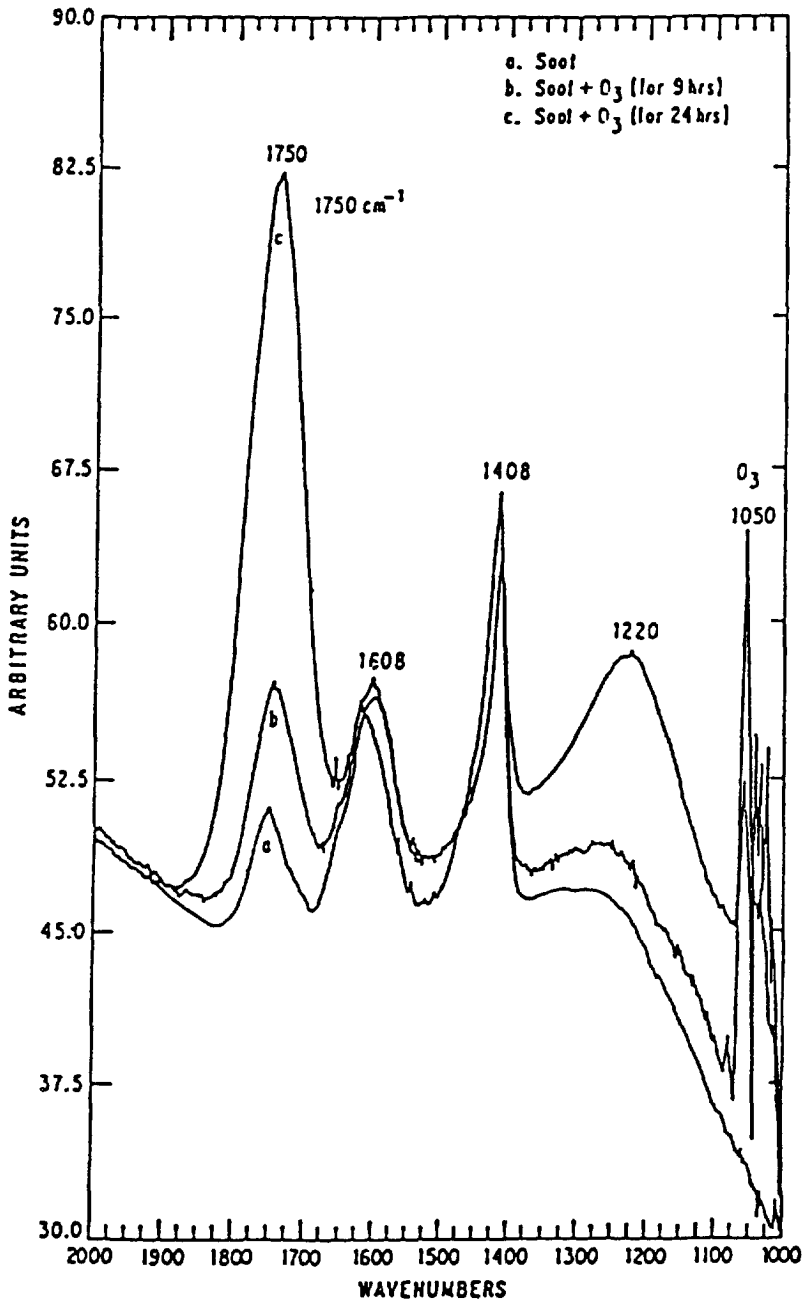

Fig. 21. Formation of oxygen-containing functionalities as a function of time. From Chughtai et al., Aerosol Sci. Technol., 15(2) (1991) 112 [66].

soluble fractions (Fig. 22), the phenomenon confirmed by the FT-IR spectra (Fig. 23).

Evidence from unpublished experiments suggests that, at very low concentrations of ozone, surface carboxylation is the primary reaction to the exclusion of others. We have determined [67] the kinetics of the ozone-hexane soot reaction, however, at ozone concentrations from 2–50 p.p.m. by

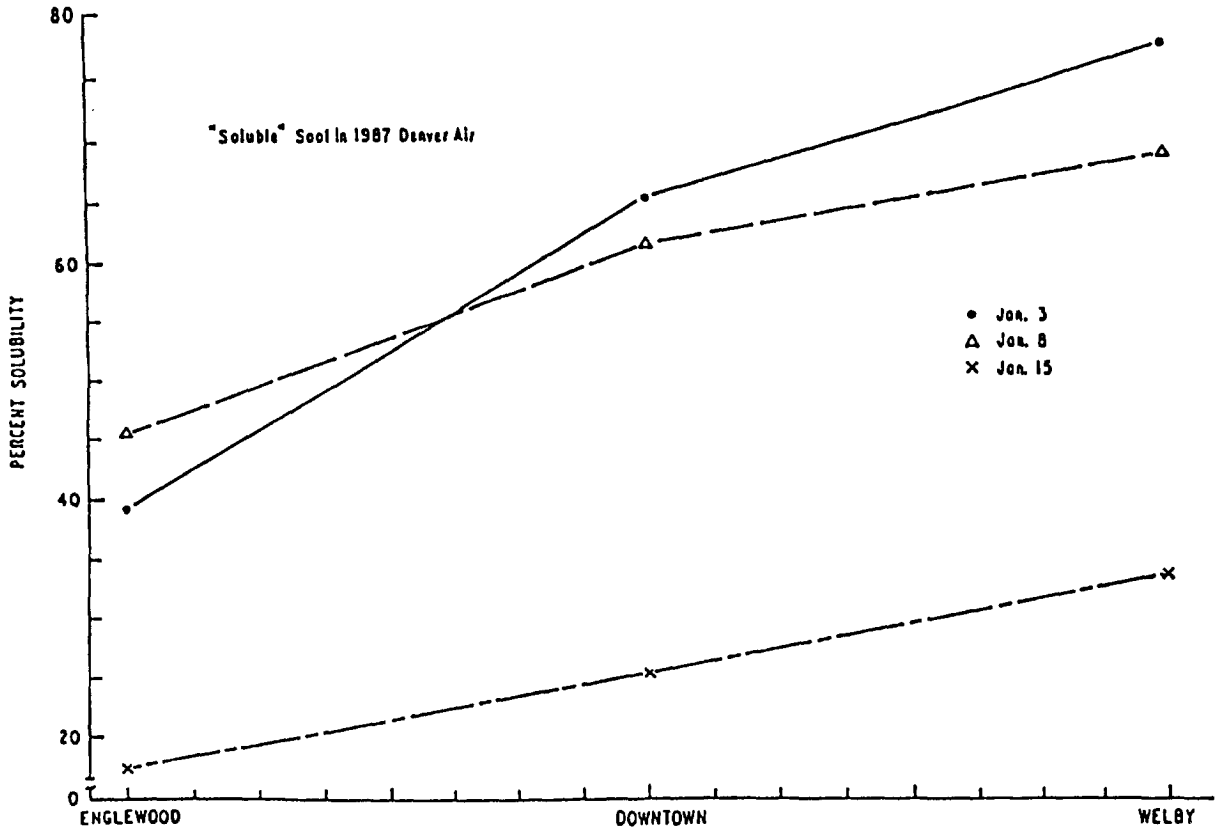

Fig. 22. The "soluble" soot in 1987 Denver air vs. collection site. From Chughtai et al., Aerosol Sci. Technol., 15(2) (1991) 112 [66].

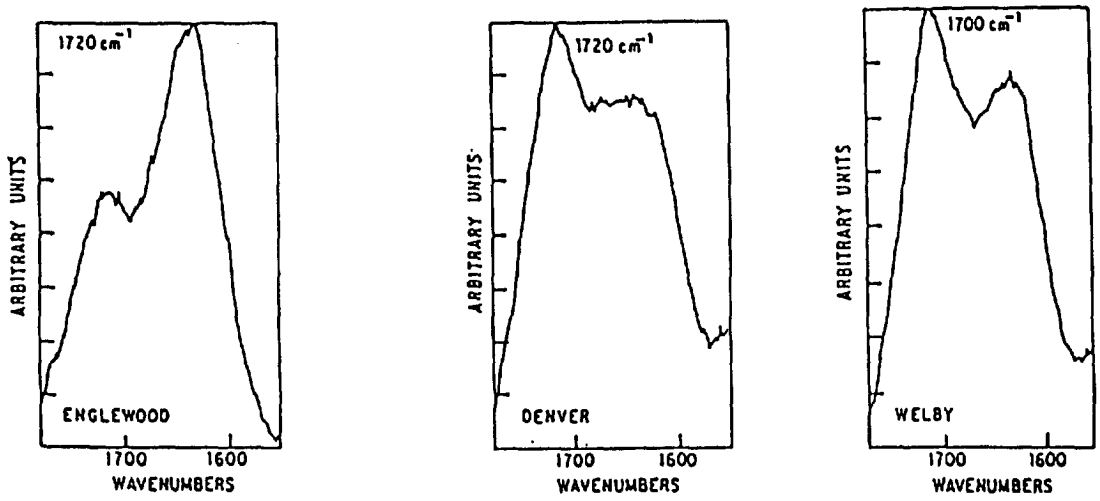

Fig. 23. FT-IR spectrum of the soluble portion of ambient particulates from three collection sites on the same date. From Chughtai et al., Aerosol Sci. Technol., 15(2) (1991) 112 [66].

means of the LOPC [Fig. 2]. At these concentrations, products CO_2 and H_2O are measureable as is the decrease in O_3 reactant concentration and, of course, the increase in soot mass by microgravimetry. Fig. 24 summarizes these measurements for one such series of experiments (15 mg soot, 23 p.p.m. O_3, 22°C). The kinetics of this reaction of black carbon appear complex but, in fact, can be conveniently separated in three stages and understood in terms of several discrete processes. Fig. 25 summarizes the three stages in terms of the diminution of reactant O_3, which are:

(i) a catalytic decomposition of O_3 upon contact with soot which occupies only the first 2% of the reaction;

(ii) a period in which surface carboxylics, CO_2 and H_2O are produced; this stage also involves a role of physisorbed O_2 [67] which is beyond the scope of discussion here;

(iii) beyond 1/3 of reaction, the rate is governed by the dissociation of O_3, presumably implicating excited O atom as the oxidizing species.

3.2.3. *Sulfur dioxide*

The behavior of sulfur dioxide in the presence of black carbon has been of interest to atmospheric chemists since the observation by Gorham [68] in 1955 of the covariance of sulfate and soot in air samples from the English Lake District. The formation of sulfate and sulfide at the surface of graphite particles exposed to SO_2 in air was demonstrated by Novakov et al. [69], as was the oxidation of SO_2 to sulfate at soot particles in the presence of water vapor. Others [70–72] have observed sulfate formation through the wet oxidation of SO_2 at carbon surfaces. The kinetics of SO_2 oxidation in aqueous solution have been worked out by Novakov and coworkers [73–76], who proposed that the carbon particle-mediated process could be a major pathway to sulfate formation in polluted airs; the conclusions of Harrison and Pio [77] are at odds with this. Infrared studies of SO_2 adsorbed on carbon films [78,79] indicated both weakly- and strongly- adsorbed species, but their characterization was uncertain. Our own research on the SO_2–black carbon system has explored mainly the effects of simulated solar radiation and carbonaceous particulate composition on the soot/SO_2/O_2/H_2O reaction system.

Fig. 26 illustrates the results of long term contact between soot and SO_2 (trace A) excluding H_2O and O_2 to the extent possible (traces remained), (trace B) in the presence of O_2 and H_2O vapor, and (trace C) after extraction of the reacted sample with water. These experiments [80] confirmed the formation of soluble sulfate from SO_2, O_2 and H_2O in the

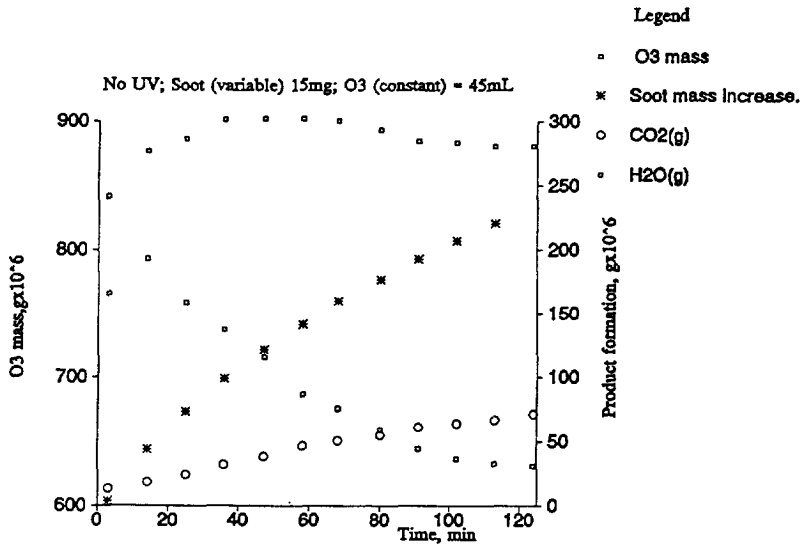

Fig. 24. Reaction of ozone with *n*-hexane soot. From Smith and Chughtai, J. Geophys. Res.-Atmos., 72 (1995) [67].

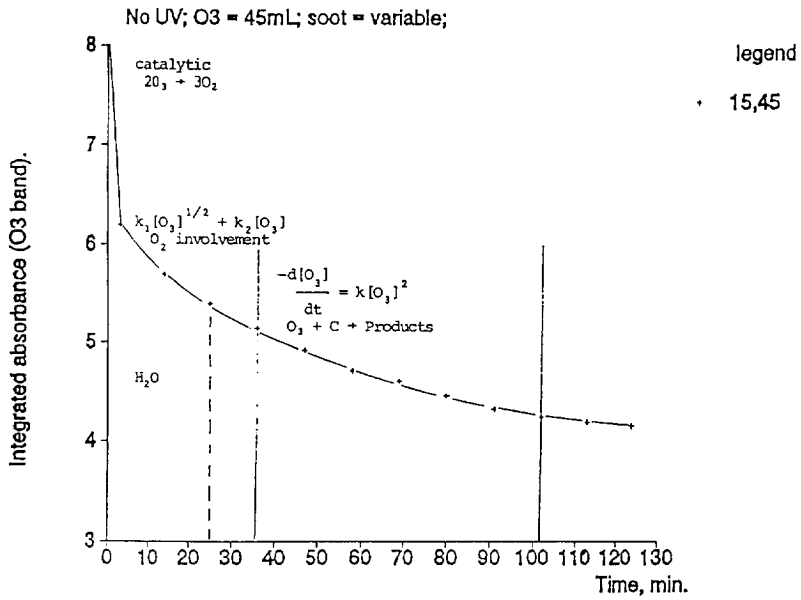

Fig. 25. Loss of ozone in the soot/O_3 reaction. From Smith and Chughtai, J. Geophys. Res.-Atmos., 72 (1995) [67].

presence of carbon, a result shown in separate experiments with sulfur dioxide-18, oxygen-18 and D_2O. Fig. 27 compares the spectrum of water-extracted soot (Fig. 26, trace C) with that of the original *n*-hexane soot. The removal of spectroscopically observable sulfate is evident, suggesting soot's catalytic role in the process.

Significant results of soot–SO_2 reactions in the presence of O_2 and water vapor under the influence of simulated solar radiation are revealed by Fig. 28 and 29. Fig. 28 is a spectrum of soot following its reaction with SO_2, O_2 and H_2O vapor, in a special quartz cell under irradiation with the solar simulator (1000 W xenon lamp, filtered to 50% at 305 nm) for 20 h. In contrast to Fig. 26, trace B, this spectrum reveals both ionic and covalent S–O-containing species formed on the carbon surface. Extraction of this solid carbon with water removes the soluble (ionic) sulfate but leaves a measurable quantity of S–O species not subject to water extraction. Fig. 29, the FT-IR spectrum following water leaching, is to be contrasted with the same region in Fig. 27. These are important results in at least two respects:

(i) they open the question of photochemically induced reactions of pollutant species in the presence of carbonaceous particles, and

(ii) they imply that the particle surface may become covered with, in this specific case, insoluble S–O species, probably diminishing any catalytic role which it may play.

Both of these conclusions currently are under study.

3.2.4. *Ongoing work*

As more complex reaction systems involving black carbon are investigated, FT-IR will continue to play a key role in the surface characterization of, and rate measurements in, these systems. Its applications will be most useful when interfaced with other techniques such as microgravimetry, thermal methods and gas chromatography. Now under study, for example, are such phenomena as particle hydration, effects of physisorbed oxygen and solar radiation, and the role of soot's unpaired electrons on adsorption and reaction rate. The hydration work is illustrative of this point. Fig. 30, a recording of mass gain as a function of increasing relative pressure of water vapor (itself increasing with time), shows the observed effect of surface

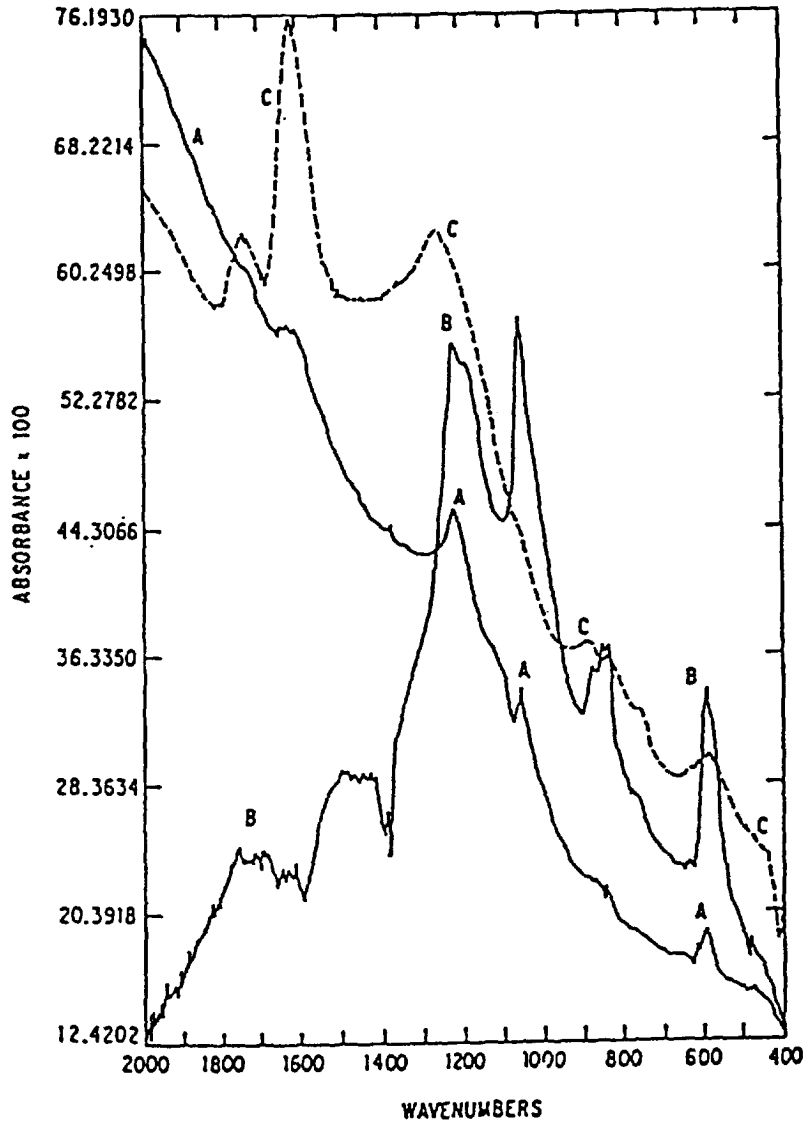

Fig. 26. Subtraction spectrum showing bisulfate bands formed on soot during soot/SO_2 reaction in the presence of water vapor and oxygen. From Smith et al., Appl. Spectrosc., 45(1) (1989) 103 (80).

oxidation on the hydration of *n*-hexane soot [81]. The direct observation of the chemisorption process at low water pressure, as mass increases are measured, is the object of the cell pictured in Fig. 31. We hope to be able to observe specific functional group interactions with water as the mass change is monitored. As one of the most definitive surface structure methods available, especially with such difficult samples as black carbon [82], FT-IR will continue to be at the center of our experimental program on the structure and reactivity of black carbon.

4. Conclusion

FT-IR spectroscopy is a powerful tool for the study of surface structure and heterogeneous reactions of black carbon. It has been applied as the

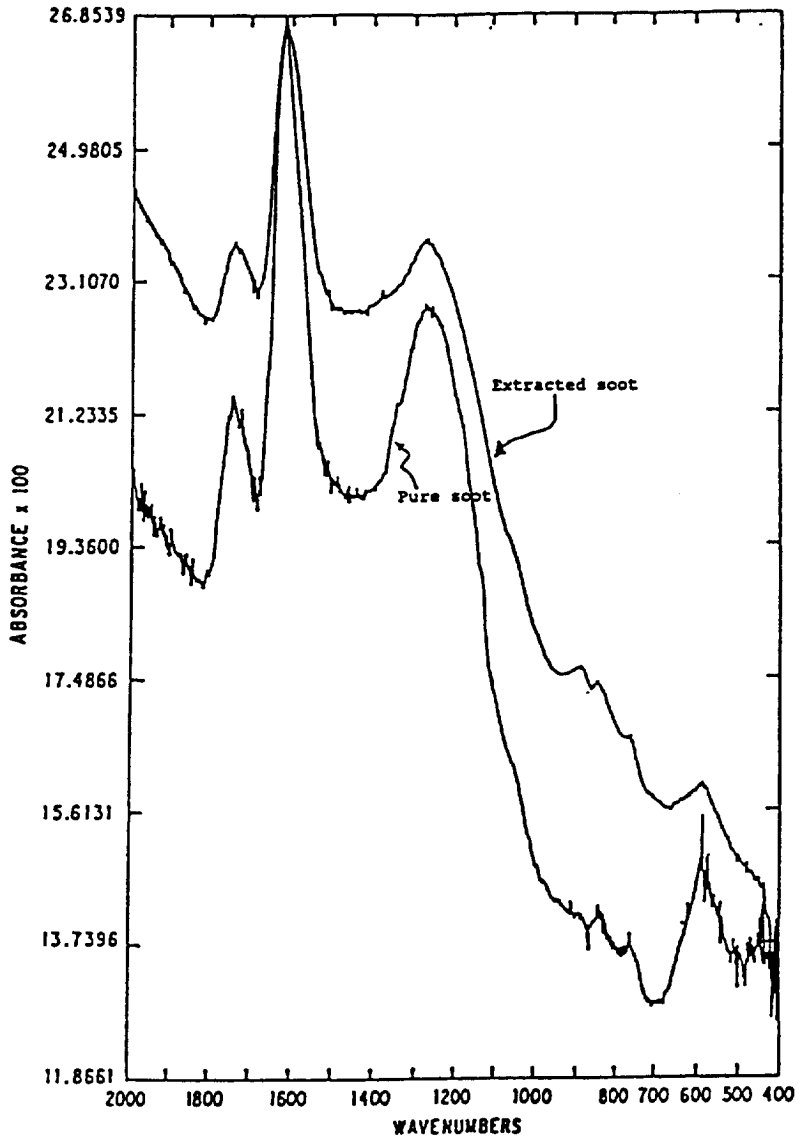

Fig. 27. The FT-IR spectrum of soot after water extraction of bisulfate formed during the soot/SO_2 reaction compared with that of original soot. From Smith et al., Appl. Spectrosc., 45(1) (1989) 103 [80].

most definitive tool in characterization of surface carbon–oxygen functionalities on *n*-hexane soot, taken as a model for carbonaceous particulate emitted by the combustion of liquid fossil fuels. Infrared data alone and acquired concomitant with isotopic substitution and thermal desorption, and in combination with several other analytical techniques, have led to a model of soot which is substantially aromatic with one-half its surface covered with oxygen-containing functionalities.

FT-IR also has proven to be the analytical method of choice for following heterogeneous reactions, including changes in surface structure and reactant/product concentrations as a function of time. Kinetics of the reactions of NO_2/N_2O_4 and ozone with *n*-hexane soot, both rapid reactions

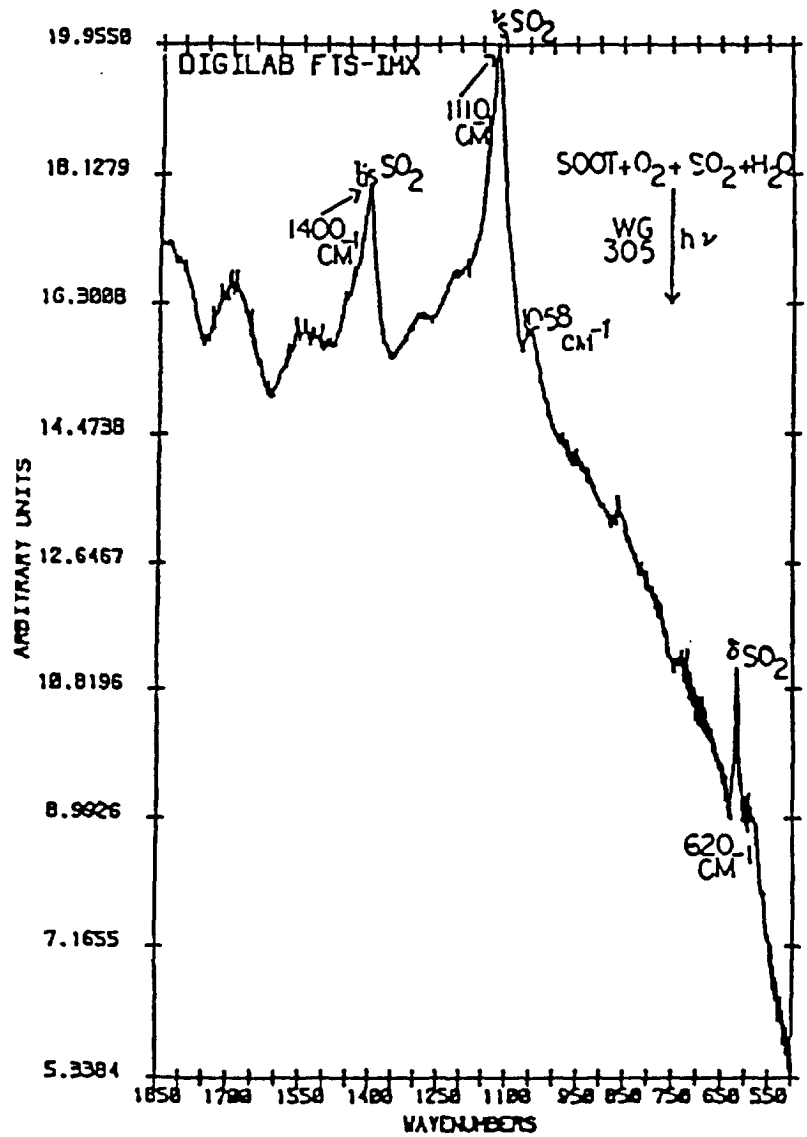

Fig. 28. FT-IR subtraction spectrum of sulfate species formed during the soot/SO_2 reaction in the presence of H_2O, O_2 and simulated solar radiation. From Smith et al., Appl. Spectrosc., 45(1) (1989) 103 [80].

(time scale in min), have revealed multipath mechanisms over a wide range of experimental conditions including concentration, temperature and exposure to simulated solar radiation. Infrared continues to be a definitive analytical tool as we explore more complex systems, including competing reactions, surface hydration, photochemically induced reactions, and the effects of physisorbed oxygen, especially as it is interfaced with other techniques such as microgravimetry.

Acknowledgement

The assistance of the National Science Foundation which provided the principal support

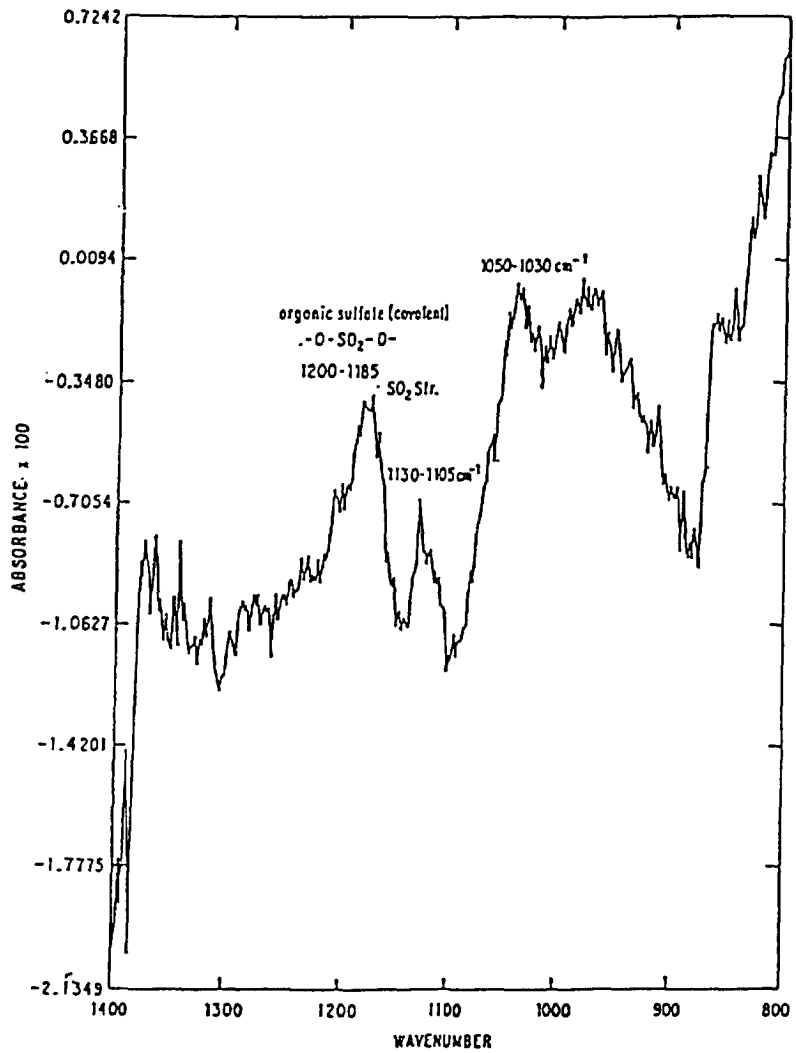

Fig. 29. FT-IR subtraction spectrum of soot following water extraction of sulfate species formed in the soot/SO_2 reaction in the presence of H_2O, O_2 and simulated solar radiation. From Smith et al., Appl. Spectrosc., 45(1) (1989) 103 [80].

of this work, through Grants MPS-7506209, ATM 8300524, ATM 8600871, ATM 88-22295 and ATM 9200923 is gratefully acknowledged. Support of the Petroleum Research Fund, through Grant 14723-ACS, and the University of Denver also is appreciated. All figures in this article bearing references are published with the permission of the authors and publishers. Numerous students and colleagues, most of whom are co-authors of articles cited herein, contributed both work and insights to this research. They include: M. Salim Akhter, Maher Atteya, Michael Brooks, Edward Goldberg, Seth Gordon, Susan Graham, John Griffin, Jabria Jassim, John Keifer, Brian Konowalchuck, Wayne McGowan, Nick Novicky, Jim Peterson, Marci Rosenberger, Chris Sergides, Don Stedman, Greory Theiss, and Bill Welch.

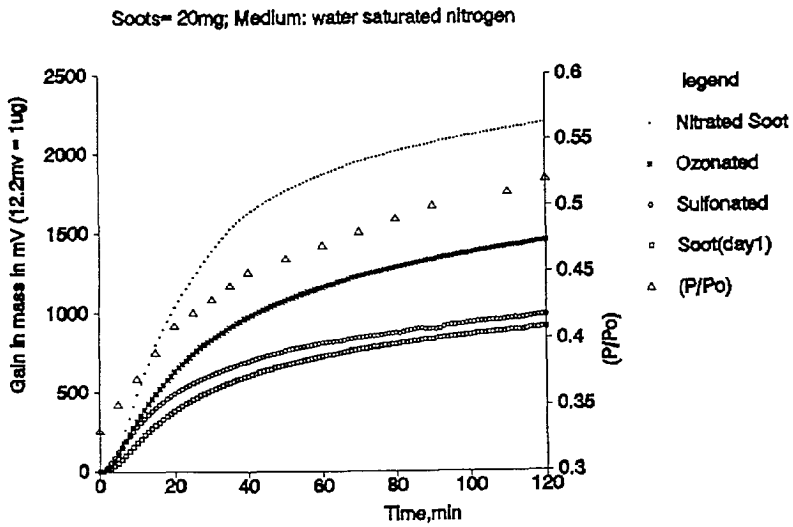

Fig. 30. Hydration of oxidized soot compared with freshly prepared soot. From Smith and Chughtai, J. Geophys. Res.-Atmos., 72 (1995) [67].

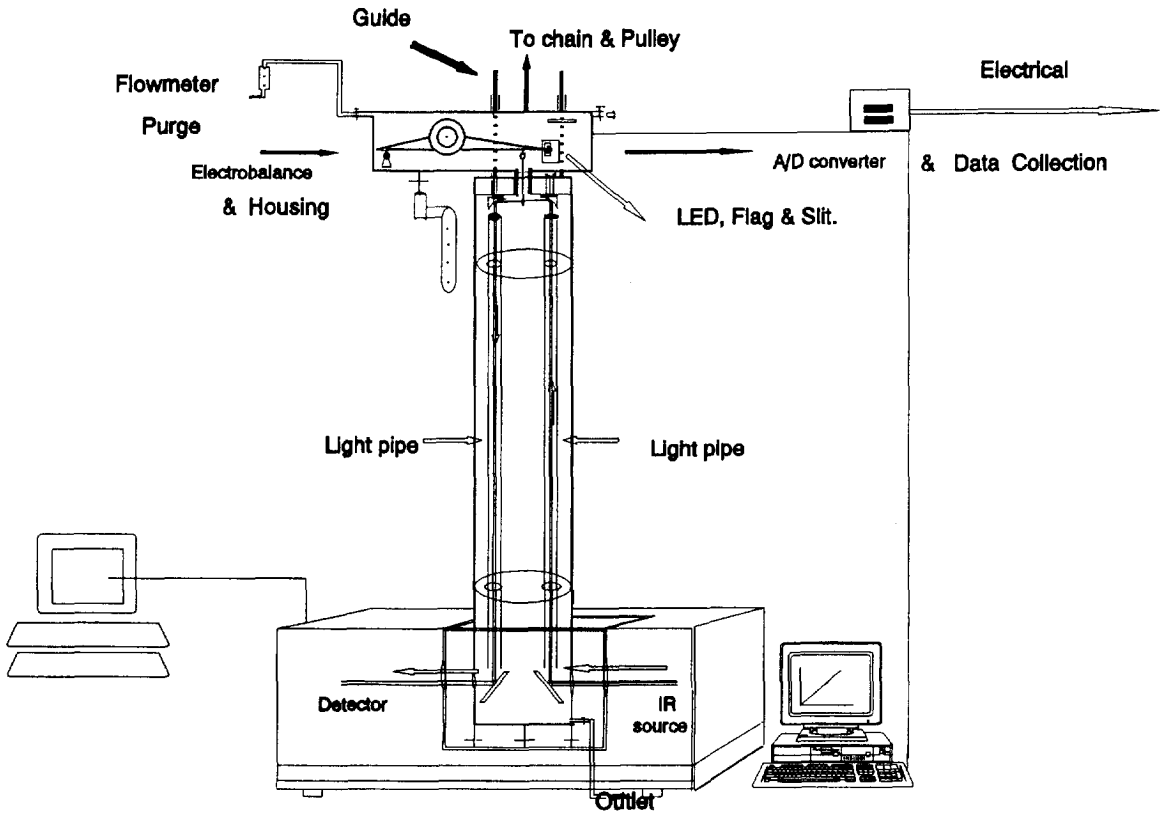

Fig. 31. Vertical LOPC interfaced with FT-IR spectrometer, electrobalance and 486PC.

References

[1] J.E. Penner, H. Eddleman and T. Novakov, Atmos. Environ., 27A(8) (1993) 1277.
[2] J.L. Muhlbaier and R.L. Williams, in G.T. Wolff and R.L. Klimisch (Eds.), Particulate Carbon: Atmospheric Life Cycle, Plenum Press, New York, 1982, pp. 185–205.
[3] R.G. Cuddihy, W.C. Griffith and R.O. McClellan, Environ. Sci. Technol., 18 (1984) 14A.
[4] E.D. Goldberg, Black Carbon in the Environment, Wiley-Interscience, New York, 1985, pp. 18–21.
[5] D.M. Smith, J.J. Griffin and E.D. Goldberg, Nature, 241 (1973) 268.
[6] H.T. Rosen, T. Novakov and B.A. Bodhaine, Atmos. Environ., 15 (1981) 1371.
[7] A.D.A. Hansen and H. Rosen, Geophys. Res. Lett., 11 (1984) 381.
[8] D.M. Smith and A.R. Chughtai, in J. Menon (Ed.), Trends in Applied Spectroscopy, Council of Scientific Research Integration, Trivandrum, India, 1994, pp. 325–365.
[9] C.G. Cannon and G.B.B.M. Sutherland, Trans. Faraday Soc., 41 (1945) 279.
[10] R.A. Friedel and J.A. Quieser, Fuel, 38 (1959) 369.
[11] V.A. Garten, D.E. Weiss and J.B. Willis, Aust. J. Chem., 10 (1957) 295.
[12] J.S. Mattson and H.B. Mark, Jr., J. Colloid Interface Sci., 31 (1969) 131.
[13] R.A. Friedel and H.L. Retcofsky, Spectrometry of Fuels, Plenum Press, New York, 1970, Chapter 5.
[14] R.A. Friedel and L.J.E. Hofer, J. Phys. Chem., 74 (1970) 2921.
[15] R.A. Friedel and L. Carlson, J. Phys. Chem., 75 (1971) 1149.
[16] D.M. Smith, J.J. Griffin and E.D. Goldberg, Anal. Chem., 47 (1975) 233.
[17] B.R. Puri, in P.L. Walker, Jr., (Ed.), Chemistry and Physics of Carbon, Marcel Dekker, New York, 1970, Chapter 3.
[18] M.L. Studebaker and R.W. Rinehart Sr., Rubber Chem. Technol., 45 (1972) 106.
[19] E. Papirer, E. Guyon and N. Perol, Carbon, 16 (1978) 133.
[20] S.G. Chang, R. Toossi and T. Novakov, Atmos. Environ., 15 (1981) 1287.
[21] J.R. Keifer, M. Novicky, M.S. Akhter, A.R. Chughtai, and D.M. Smith, SPIE J., 289 (1981) 184–188.
[22] M.G. Rockley, A.E. Ratcliffe, D.M. Davis, and M.K. Woodard, Appl. Spectrosc., 38 (1984) 553.
[23] R.T. Lynch, A.R. Chughtai and D.M. Smith, Amer. Lab., 1995, in press.
[24] D.M. Smith, M.S. Akhter, C.A. Sergides, J.A. Jassim, W.F. Welch, and A.R. Chughtai, Aerosol Sci. Technol., 10 (1989) 311.
[25] M.S. Akhter, A.R. Chughtai and D.M. Smith, Appl. Spectrosc., 39(1) (1985) 143.
[26] A.R. Chughtai and D.M. Smith, Appl. Spectrosc., 45(7) (1991) 1204.
[27] D. Lin-Vien, N.B. Colthup, W.G. Fateley, and J.G. Grasselli, The Handbook of Infrared and Raman Characteristic Frequencies of Organic Molecules, Academic Press, Inc., San Diego, 1991, pp. 61–64, 284–287.
[28] E. Fitzer, K. Muller and W. Schueffer, in P.L. Walker, Jr., (Ed.), Chemistry and Physics of Carbon, Marcel Dekker, Inc., New York, 1971, Chapter 5.
[29] J.A. Jassim, H.P. Lu, A.R. Chughtai, and D.M. Smith, Appl. Spectrosc., 40 (1986) 113.
[30] G.P. Scott and D.S. Tarbell, J. Am. Chem. Soc., 72 (1950) 240.
[31] H.P. Koch, J. Chem. Soc., (1951) 512.
[32] R.R. Gordon, W.N. Adams and G.I. Jenkins, Nature, 170 (1952) 317.
[33] C.G. Cannon, Nature, 171 (1953) 308.
[34] R.A. Friedel and M.G. Pelipetz, J. Opt. Soc. Am., 43 (1953) 1051.
[35] D.J. Brake and E.R. Cole, J. Appl. Chem., 5 (1955) 477.
[36] J.K. Brown, J. Chem. Soc. (London), 1 (1955) 744.
[37] H.A. Van Vucht, B.J. Rietveld and D.W. Van Krevelen, Fuel, 35 (1955) 50.
[38] M. Ceh and D. Hadzi, Fuel, 35 (1956) 77.
[39] R.A. Friedel and J.A. Quieser, Anal. Chem., 28 (1956) 22.
[40] J.D. Brooks, R.A. Durie, B.M. Lynch and S. Stephnell, Aust. J. Chem., 13 (1960) 179.
[41] B.R. Puri, 5th Carbon Conference, Pennsylvania State University, 23 June 1961. Vol. 2, Pergamon Press, New York, 1962–1963, p. 160.
[42] H.S. Rao, P.L. Gupta, F. Kaier and A. Lahiri, Fuel, 41 (1962) 417.
[43] L. Czuchajowski and G.J. Lawson, Fuel, 42 (1963) 131.
[44] S. Fujii, Fuel, 42 (1963) 17.
[45] S. Fujii, Fuel, 42 (1963) 341.
[46] S. Fujii and H. Tsuboi, Fuel, 46 (1967) 361.
[47] K.H. Ludlum and R.P. Eischens, Div. Petr. Chem., Am. Chem. Soc., (1976) 375.
[48] C. Morterra and M.J.D. Low, Spectrosc. Lett., 159 (1982) 689.
[49] M.L. Josien and N. Fuson, J. Am. Chem. Soc., 73 (1971) 478.
[50] R.A. Nyquist, Appl. Spectrosc., 36 (1982) 533.
[51] G.E. Maciel, V.J. Bartuska and F.P. Miknis, Fuel, 58 (1979) 391.
[52] H.L. Retcofsky, J.M. Stark and R.A. Friedel, Anal. Chem., 40 (1968) 1699.
[53] T.F. Yen, J.G. Erdman and S.S. Pollack, Anal. Chem., 33 (1961) 1587.
[54] T.F. Yen, J.G. Erdman and A.J. Saraceno, Anal. Chem., 34 (1962) 694.
[55] M.S. Akhter, A.R. Chughtai and D.M. Smith, Appl. Spectrosc., 39(1) (1985) 154.
[56] C.A. Sergides, J.A. Jassim, A.R. Chughtai, and D.M. Smith, Appl. Spectrosc., 41(3) (1987) 482.
[57] M.S. Akhter, A.R. Chughtai and D.M. Smith, J. Phys. Chem., 88 (1984) 5334.

[58] D.O. Hayward and B.M.W. Trapnell, Chemisorption, Butterworths, London, 1964, pp. 93.
[59] A.R. Chughtai, S.A. Gordon and D.M. Smith, Carbon, 32(3) (1994) 405.
[60] B.J. Finlayson-Pitts and J.N. Pitts, Jr., Atmospheric Chemistry: Fundamentals and Experimental Techniques, John Wiley and Sons, New York, 1986, p. 151.
[61] D.M. Smith, W.F. Welch, S.M. Graham, A.R. Chughtai, B.G. Wicke, and K.A. Grady, Appl. Spectrosc., 42 (1988) 647.
[62] B.G. Wicke and K.A. Grady, Combust. Flame, 66 (1986) 37.
[63] A.R. Chughtai, W.F. Welch and D.M. Smith, Carbon, 28(2/3) (1990) 411.
[64] M.S. Akhter, A.R. Chughtai and D.M. Smith, Carbon, 23 (1985) 593.
[65] P.R. Steckel and R.B. Engdahl, Encyclopedia of Chemical Technology, 3rd edn., Wiley-Interscience, New York, 1978, pp. 624–669.
[66] A.R. Chughtai, J.H. Peterson, J.A. Jassim, D.H. Stedman, and D.M. Smith, Aerosol Sci. Technol., 15(2) (1991) 112.
[67] D.M. Smith and A.R. Chughtai, J. Geophys. Res.-Atmos., 72 (1995), in press.
[68] E. Gorham, Geochim. Cosmochim. Acta, 7 (1955) 321.
[69] T. Novakov, S.G. Chang and A.B. Harker, Science, 186 (1974) 259.
[70] L.D. Hulett, T.A. Carlson, B.R. Fish, and J.L. Durham, in G. Mamantov and W.D. Shults (Eds.), Determination of Air Quality, Plenum Press, New York, 1972, pp. 179–187.
[71] A.C. Baldwin, Int. J. Chem. Kinet., 14 (1982) 269.
[72] R. Dlugi and H. Gusten, Atmos. Environ., 17 (1983) 1765.
[73] R. Brodzinsky, S.G. Chang, S.S. Markowitz, and T. Novakov, J. Phys. Chem., 84 (1980) 3354.
[74] S.G. Chang, R. Brodzinsky, R. Toossi, S.S. Markowitz, and T. Novakov, Proc. Conference on Carbonaceous Particles in the Atmosphere, Report No.LBL-903Z, Lawrence Berkeley Laboratory, CA, 1979.
[75] S.G. Chang, R. Toossi and T. Novakov, Atmos. Environ., 15 (1981) 1287.
[76] S.G. Chang and T. Novakov, Adv. Environ. Sci. Technol., 12 (1983) 191.
[77] R.M. Harrison and C.A. Pio, Atmos. Environ., 17 (1983) 1261.
[78] J. Zawadzki, Carbon, 25(3) (1987) 431.
[79] J. Zawadzki, Carbon, 25(4) (1987) 495.
[80] D.M. Smith, J.R. Keifer, M. Novicky, and A.R. Chughtai, Appl. Spectrosc., 43(1) (1989) 103.
[81] A.R. Chughtai, M.E. Brooks and D.M. Smith, J. Geophys. Res.-Atmos, 72 (1995), in press.
[82] M.S. Akhter, A.R. Chughtai and D.M. Smith, Appl. Spectrosc., 54(4) (1991) 653.